REPUBLIC OF TÜRKİYE

ALTINBAŞ UNIVERSITY

Institute of Graduate Studies

Architecture Department

POINT CLOUD SEMANTIC SEGMENTATION OF BUILDING ELEMENTS OF FATIH MOSQUE, ISTANBUL

Khwlah KASEM AGHA

Master's Thesis

Supervisor

Asst. Prof. Dr. Can UZUN

İstanbul, 2024

POINT CLOUD SEMANTIC SEGMENTATION OF BUILDING ELEMENTS OF FATIH MOSQUE, ISTANBUL

Khwlah KASEM AGHA

Architecture Department

Master's Thesis

ALTINBAŞ UNIVERSITY

2024

The thesis titled POINT CLOUD SEMANTIC SEGMENTATION OF BUILDING ELEMENTS OF FATIH MOSQUE, ISTANBUL prepared by KHWLAH KASEM AGHA and submitted on 05/12/2024 has been **accepted unanimously** for the degree of Master of Science in Architecture.

Asst. Prof. Dr. Can UZUN
Supervisor

Thesis Defense Committee Members:

Asst. Prof. Dr. Can UZUN	Department of Architecture, Altınbaş University	_____
Asst. Prof. Dr. Erinç ONBAY	Department of Interior Architecture and Environmental Design, Altınbaş University	_____
Asst. Prof. Dr. Derya KARADAĞ	Department of Interior Architecture and Environmental Design Işık University	_____

I hereby declare that this thesis meets all format and submission requirements for a master thesis.

I hereby declare that all information/data presented in this graduation project has been obtained in full accordance with academic rules and ethical conduct. I also declare all unoriginal materials and conclusions have been cited in the text and all references mentioned in the Reference List have been cited in the text, and vice versa as required by the abovementioned rules and conduct.

Khwlah KASEM AGHA

Signature

DEDICATION

I would like to dedicate this thesis to my parents, Msef and Turfah, my siblings Osama, Amin, Rajaa, and my life partner Rani, for their unconditional love and support. Thank you to my parents, who stood by my side and provided me with strength and inspiration to walk through each step of this process. To my partner and siblings, who were the source of my motivation and encouragement. To my supervisor, Architect. Abdel Wahab Antar, who encouraged me to continue my studies and shared with me his valuable knowledge. To my advisor, thank you for your invaluable guidance and insights. I am grateful for the experiences that helped shape my research and work.

ABSTRACT

POINT CLOUD SEMANTIC SEGMENTATION OF BUILDING ELEMENTS OF FATIH MOSQUE, ISTANBUL

KASEM AGHA, Khwlah

M.Sc., Architecture Department, Altınbaş University,

Supervisor: Asst. Prof. Dr. Can UZUN

Date: 12/2024

Pages: 95

Creating digital models for heritage buildings is important for preserving a city's history and identity. The Fatih Mosque in Istanbul, a vulnerable historical landmark, was subjected to multiple strong earthquakes over the years, highlighting the need for long-term conservation strategies. Despite its significance and need for conservation solutions, there is limited literature on the protection of mosques, particularly in the use of technology for the documentation and conservation of mosques. This study focuses on the digital documentation and autonomous detection of the captured elements from the Fatih mosque's facades, using semantic segmentation of a point cloud model for the detection and classification of the facades' elements. The point cloud data was captured through a photogrammetric approach using a smartphone camera, documenting the southwestern and northwestern facades. The captured data was processed in Agisoft Metashape software for the point cloud model generation and classified using the CANUPO classifier within CloudCompare software to segment the facades' elements. Classification results demonstrated moderate but considerable outcomes on the CANUPO's classifier ability to detect heritage building elements. Results also showed good potential in utilizing smartphones for generating digital heritage point cloud models. With further refinements and developments, this study provides a valuable technological framework for the documentation and preservation of Fatih Mosque, offering new insights into the application of digital tools in heritage conservation.

Keywords: Heritage Digital Models, Point Cloud Models, Semantic Segmentation, Photogrammetry, CANUPO Classifier, Fatih Mosque.

TABLE OF CONTENTS

Pages

LIST OF TABLES

Pages

LIST OF FIGURES

Pages

LIST OF CHARTS

Pages

ABBREVIATIONS

AEC	:	Architecture – Engineering – Construction
ALS	:	Airborne Laser Scanner
BIM	:	Building Information Modeling
FN	:	False Negatives
FP	:	False Positives
FPR	:	False Positive Rate
GTP	:	Ground Truth Points
HBIM	:	Heritage Building Information Modeling
MLS	:	Mobile Laser Scanner
PCSS	:	Point Cloud Semantic Segmentation
SOR	:	Statistical Outlier Removal
TLS	:	Terrestrial Laser Scanner
TN	:	True Negatives
TP	:	True Positives
UAVs	:	Unmanned Ariel Vehicles

1. DIGITAL REPRESENTATION OF ARCHITECTURAL HERITAGE

Heritage preservation is a widely researched topic, which is vital for preserving cities' identities and cultures. Historical buildings also referred to as heritage buildings, are buildings built in the past that portray historical events and stories of the time it was built in (Penjor et al., 2024). Also, some historical buildings are built as memorials for past events or for people who participated in a historical event, to pass their stories to future generations. These assets are important because they resemble past stories, events, and traditions that creates the city's character. Once these historical buildings are lost, the identities and stories that they portray cannot be returned (Solla et al., 2020). Therefore, examining the conditions of historical buildings regularly and checking for needed renovations or alterations is essential for their protection and conservation (Martinelli et al., 2023) (Stober et al., 2018). These assessments include evaluating the general building condition, observing buildings' material types and quantities, analyzing structural elements' condition, checking for cracks and damages, and deciding whether to repair or alter (Solla et al., 2020). Usually, assessing heritage structures relies on using traditional methods in the initial stage to gather information about the historical structure and to produce the needed documents. These methods require the intervention of a surveyor who visits the site multiple times, determines key points, takes notes on any visible damage, takes measurements, and then manually converts the collected data and measured distances into CAD software to produce 2D drawings including plans, sections, and elevations. Then, these documents can be further developed in 3D modeling software, which requires modeling of the historical building from scratch. However, this process is inconvenient because heritage buildings have so many details, complex ornaments, and geometries that are hard to manage and recreate manually. Consequently, using traditional methods for documentation and preservation is tedious and a time-consuming procedure (Baik, 2017).

1.1 DIGITAL MODELS OF HERITAGE BUILDINGS

As a better alternative to traditional methods for the data collection and representation of heritage buildings, utilizing three-dimensional (3D) digital heritage models of heritage buildings became essential. Recent studies note that implementing advanced technology with heritage buildings is very effective and beneficial on multiple aspects like the

documentation and preservation of historical assets (He et al., 2017). Digital heritage models communicate the need to preserve the cities' identities and cultures (Champion & Rahaman, 2019). Digital heritage models are a replication of existing historical structures which acts as a reliable and sharable data source, that can be utilized in 2D and 3D software to obtain needed documents (Grilli & Remondino, 2019) (Maiwald et al., 2019). Penjor et al. (2024) explained heritage digital representations as an emerging approach that combines the use of technology and advanced tools with existing heritage buildings, to recreate and document all stages of the existing project. Digital heritage models can be represented in the form of meshes or point cloud models. It is a worldwide adapted tool used by different sectors such as architects, and electrical, mechanical, and structural engineers which is useful for evaluation, analysis, and observation (Grilli & Remondino, 2019). A typical architectural project workflow usually starts with conceptual sketching and ends with 3D renders developed using modeling and rendering software, where the use of technology usually ends after the construction phase ends. However, for digital heritage models, the opposite workflow is followed where the use of advanced technology is important and helpful after the construction phase ends.

Heritage digital models play an important role in their implementation within different sectors like tourism, virtual reality VR, augmented reality AR, and heritage preservation. Poux et al., (2020), produced a digital model of Jehay's castle in Belgium to perform a VR tour showcasing the castle and promoting a multi-use immersive experience. Within the historical preservation sector, capturing and replicating an existing building and its elements increases the efficiency of decision-making concerning alteration, maintenance, and restoration (Pocobelli et al., 2018). Also. it enables the observation of the structure to monitor id any damage occurred or might happen in the future (Mol et al., 2020). Moreover, it provides a digital archive of the existing structure that can be accessed at any time for assessment and observation. The archives can be shared, analyzed, and developed, enabling the creation of 2D drawings consisting of plans, sections, and elevations along with 3D presentations showing the interior and exterior elements. Most importantly digital heritage representation offers great benefits for the heritage conservation sector, as shown in (Figure 1.1), the acquired benefits include documentation, representation, classification of building elements, and the integration within heritage building information modeling HBIM (Clini et

al., 2024) (Nespeca et al., 2024) (Shabani et al., 2022) (Costantino et al., 2021) (Bacci et al., 2019) (Baik, 2017b).

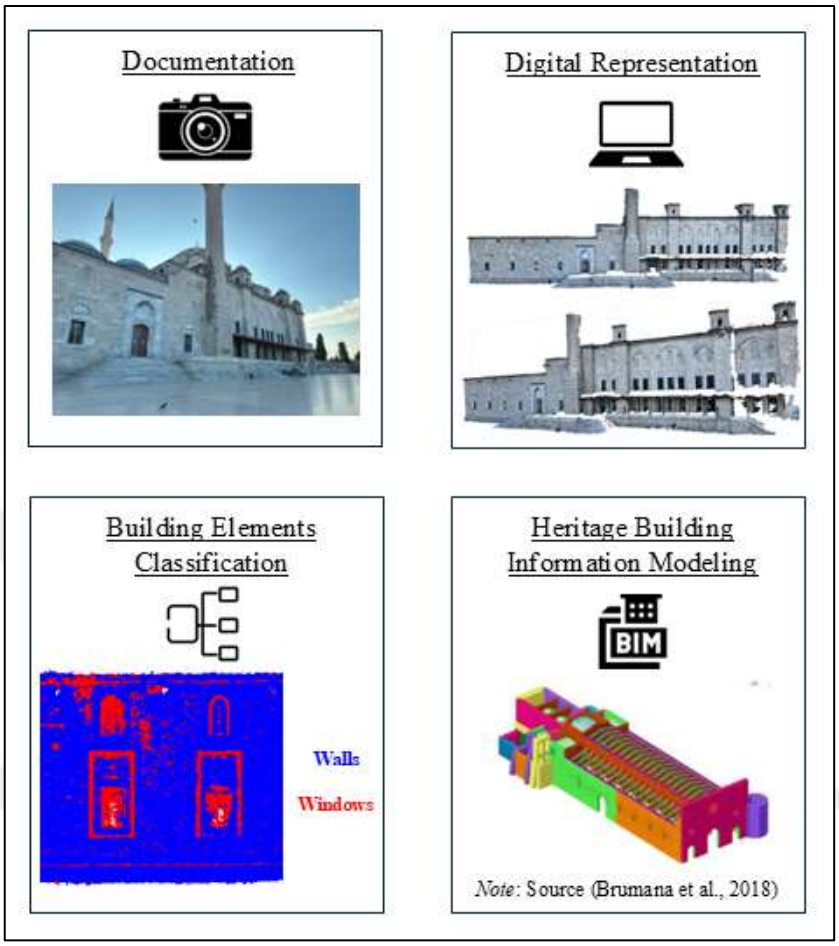

Figure 1.1: Importance of Digital Models for Heritage Conservation.

Regarding the mentioned benefits, the efficiency of the decision-making process concerning renovation, maintenance, and evaluation increases (Truong-Hong & Lindenbergh, 2022) (Croce et al., 2021) (Pocobelli et al., 2018) (Macher et al., 2017). As Capone and Lanzara (2019) note, digital replicas of heritage buildings allow for detailed assessment and refinement through the generation of a sharable digital model.

Many studies highlighted their importance and usability in various contexts. (Baik, 2017) focused on the digital documentation of a heritage house in Jeddah, Saudi Arabia. They produced a heritage representation model to add to Jeddah's heritage database where information is stored on which buildings need to be preserved, restored, or completely removed. Another study by Psomadaki et al. (2018), involved different professionals in the

production of a model which contributed to the management and documentation of heritage structures. They mentioned that these studies promote the production of smart digital cities. Additionally, most studies on digital heritage are associated with their implementation within building information modeling (BIM) software, referred to as Heritage BIM (HBIM). HBIM is a branch of the broader BIM domain, that specializes in generating a digital representation model of a heritage building and implementing it in BIM software like Revit (Themistocleous et al., 2022). Colucci et al. (2020) experimented with merging HBIM with GIS data to fill the needed notes for the restoration and conservation of a church in Italy that was subjected to multiple earthquakes. The results showed a good level of interoperability between HBIM and GIS data.

Further studies need to explore digitalizing historical buildings from all around the world, capturing buildings from different eras with different architectural languages. In the case of historical assets within Turkey, several studies explored the digitalization of its heritage mosques and buildings (Agirbas et al., 2022) (Bianchini, 2020) (Kan et al., 2019) (Benli, 2015). Bianchini (2020) generated a point cloud model of the main dome and piers of the Hagia Sophia mosque to perform surveys on the dome's structure. Another beneficial study aimed at Istanbul's heritage preservation (Kan et al., 2019), who used a laser scanner with a panoramic camera to capture the Suleymaniye mosque, and produced a point cloud model then remodeled it in 3Ds Max program to utilize it for virtual tours. Moreover, Kan et al. (2019), used a laser scanner with a panoramic camera to capture the Suleymaniye mosque, with the purpose of digitalization and using the digital model for VR tours. Another study produced a digital model for Fatih Street within the historic peninsula using Terrestrial Laser Scanning (TLS) for data collection (Benli, 2015), and Agirbas et al. (2022) extracted the muqarnas elements from the main gate of Sehzade, Suleymaniye, and Atik Valide Mosques for semantic segmentation. Despite these efforts, the Fatih mosque has received little attention in the literature concerning its conservation, even though it is one of Istanbul's significant historical buildings. Therefore, this study focuses on creating a digital record of the Fatih mosque, which was built between 1462 and 1470 and designed by the Architect Atik Sinan. Through the development of a point cloud model and classifying the mosque's elements using semantic segmentation.

1.2 FATIH MOSQUE HISTORICAL SIGNIFICANCE AND PRESERVATION NEEDS

Fatih mosque as shown in (Figure 1.2), is a UNESCO World Heritage site located in the historical Fatih district in Istanbul/ Turkey. In 1462, after Istanbul was conquered, the Fatih mosque was built and named after the conqueror Fatih Sultan Mehmet II on a high hill with a grand architectural complex consisting of surrounding buildings like schools, hospitals, and kitchens, forming one of the most remarkable historical monuments in Istanbul (Kunter & Ülgen, 1939, p. 1).

Figure 1.2: Fatih Mosque in Istanbul / Türkiye.

Its historical importance goes back to its original structure, which collapsed but it resembled the Turkish identity and Ottoman architectural style that evolved within Istanbul. Originally, the construction work started in 1462. However, the original structure was lost because it faced major structural threats over the centuries due to its exposure to multiple strong earthquakes. According to Durukal et al. (2001), the Fatih mosque is the most affected heritage building in Istanbul by natural events, particularly earthquakes. In 1509, a strong earthquake named the "Little Apocalypse" damaged the main dome and the columns' capitals. Repeatedly, parts of the mosque were damaged in 1557 and 1754 because of the earthquakes that occurred. Moreover, in 1765, the structure couldn't endure the devastating earthquake which caused the main dome and supporting wall to collapse beyond repair (Kunter & Ülgen, 1939, p. 1), this led to the involvement of an architect named Eski Sinan, which the reconstruction started in 1767 and ended in 1771. As shown in (Figure 1.3) the

1765 earthquake caused major reconstruction that altered the Fatih mosque's original plan different from the existing plan (Bal et al., 2015) (Kunter & Ülgen, 1939). Additionally, after the 1999 earthquake, studies claim that the mosque might be exposed to severe collapses again because of its close distance to a major fault (Bal et al., 2015).

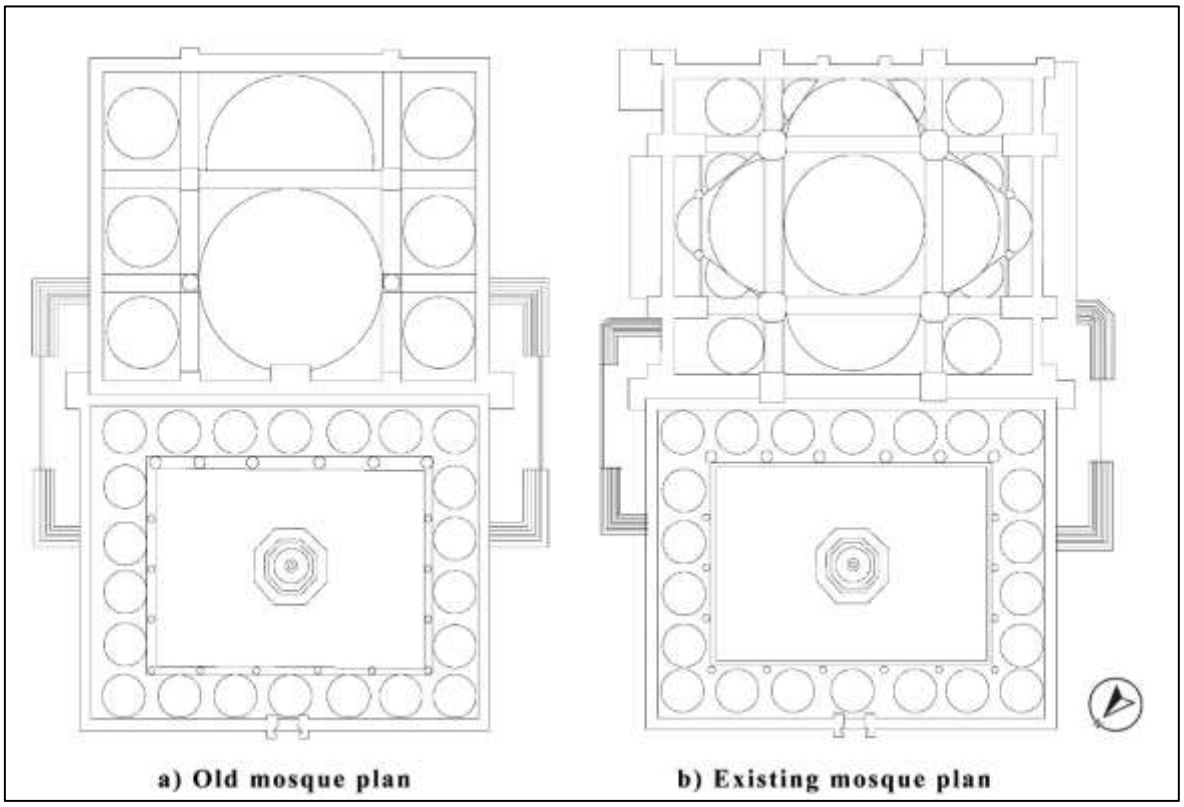

Figure 1.3: Plan Schemes of the Fatih Mosque in Istanbul.

Figure 1.3 displays (a) the original plan before the mosque collapsed, and (b) the existing plan after it was reconstructed on the same land. Originally, the mosque had two semi-square spaces of an open courtyard and a prayer hall. It had an unsymmetrical plan layout with a main dome of 26 meters in diameter and a semi-dome on one side at the same level with six smaller domes on a lower level (Bal et al., 2015). According to Vatan (2018), one of the main causes of the original mosque collapse is the unsymmetric plan design. Plan (b) of the existing mosque has a smaller dome of 19 meters surrounded by semi-domes on four sides. The main dome rests on four arches, supported by four pillars to provide an equal load distribution system.

In the original mosque, the Turkish architectural elements were portrayed mainly in its minarets and domes representing early classical Ottoman architecture, where the façade

elements of rectangular windows, pointed arch windows, columns, and doorways were more regular and in harmony, as seen in (Figure 1.4) referenced from (Kunter & Ülgen, 1939) book.

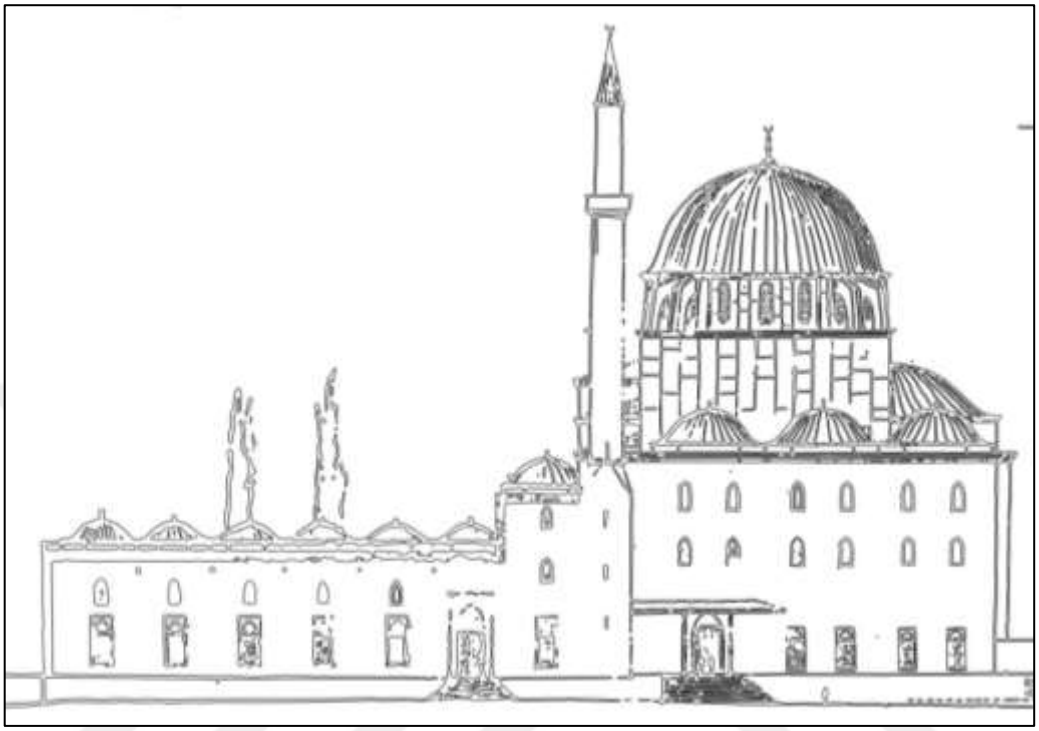

Figure 1.4: Elevation of the Old Fatih Mosque, Before it Collapsed.

The existing mosque has a simpler and more static style, where the facade elements have more ornaments and stone carvings influenced by the baroque style (Kunter & Ülgen, 1939, p. 5), merging two styles into one historical monument. Upon limited literature, some historians concluded from ancient writing that the mosque was built on the location of a preexisting church named Havarion Church in the Byzantine era, which influenced the existing mosque style, however, no concrete literature links it to the mosque, as some suggest that it was only close to it and not built on the same site (Kunter & Ülgen, 1939, p. 6). However, this didn't affect the original aesthetic in which the Turkish ottoman style remained. Regarding the current mosque's façades and exterior elements, the mosque features two minarets, each with three balconies, built from stone and marble. Moreover, it features multiple wooden entrances, three leading to the open courtyard and three leading directly to the prayer hall. Several common design features are employed within mosques built in the Ottoman era, including the main dome placement on a higher level, rectangular

lower windows, upper pointed arched windows, open courtyards enclosed by corridors shaded with small domes, and richly decorated gates with muqarnas elements, as illustrated in (Figure 1.5) referenced from (Gurlitt, 1912) book. These design elements are repeated on multiple mosques within Istanbul, which yields to the importance of digitalizing and semantically segmenting the mosque's elements to produce an automatic digitalization and segmentation approach for all the mosques with the same style.

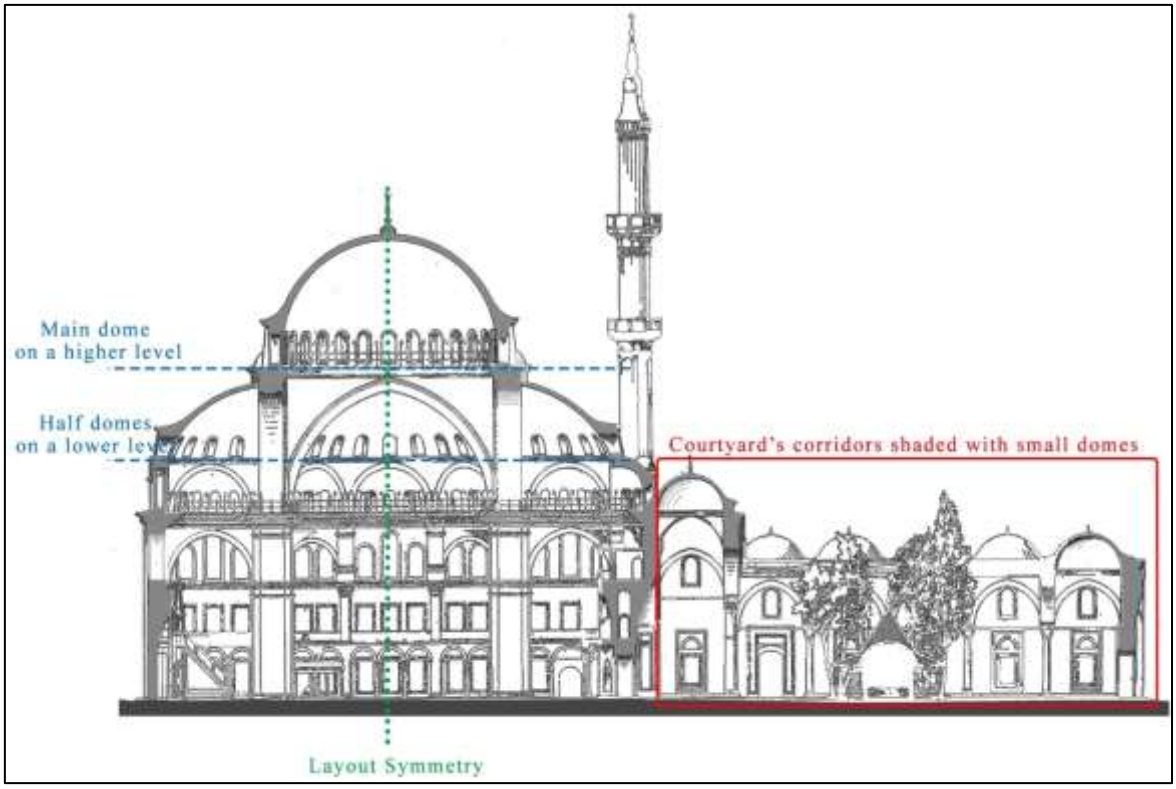

Figure 1.5: Section of the Existing Fatih Mosque.

Measured in Google Earth, the main northwestern facade of the open courtyards is 60 meters long. It features 6 lower rectangular windows, 6 upper pointed arch windows, and one main marble entrance that leads directly to the courtyard. This Marble entrance, influenced by Seljuk architecture, remained even after the earthquake occurrence. It was acknowledged by historians because it resembles the victory of the Turkish army where they passed and stood showing power and unity (Kunter & Ülgen, 1939, p. 1). This landmark doesn't only resemble beauty, but it further conveys strength and historical accomplishments. The other long facades, which are the southwestern and northwestern facades are 95 meters long, with 28 rectangular windows, 17 upper pointed arch windows, and two wooden entrances, one leads

to the courtyard, and the other leads to the prayer hall. While the northeastern side has 19 rectangular windows and 24 pointed arch windows with no entrances, this side can't be accessed and fully seen because it has a graveyard with the tombs of Sultan Mehmed II and his consort Gülbahar Hatun tombs, also it has the domed Carullah Efendi Library in front of it.

Because the mosque's structural integrity is at constant risk, several researchers conducted studies on the causes and solutions behind the mosque's structural weakness and multiple collapses. (Vatan, 2018) studied structural problems related to the cause of big damage that altered the original structure. They concluded that the main issue within the old structure lies in its thin, slender masonry walls and asymmetrical plan design. However, this study required the intervention of multiple sophisticated programs to conclude this outcome. On a more detailed aspect, Akyuz et al. (2015) analyzed the type of plaster and mortar used in Fatih mosque's wall painting materials. A partial sample from the main dome was taken and analyzed using a combination of EDXRF micro-Raman and FTIR which are techniques that measure different material radiation from a building element sample. Conducting this helped in understanding the nature of the building's raw materials. For documentation purposes, (Yastıklı & Alkı) used a photogrammetry and remote sensing approach to capture the façade of Fatih mosque. The captured photos were used to generate stereo photographs, which were transformed into 3D vector data, achieved manually by a specialized operator. Even though the model was produced, the manual modeling of the façade required a professional to do it and it consumed long periods, contrary to the use of advanced technology that can produce the same model but in a significantly shorter amount of time. (Beyen, 2008) reported the results from the structural identification and analysis during an earthquake that occurred in 1999. With multiple detailed structural models, the study aimed at conserving the mosque by identifying current structural problems and the prediction of structural responses to any future earthquakes. (Berilgen, 2007), conducted an in-depth analysis of the soil condition and structural behavior during past earthquakes along with the prediction of its future behavior. Table 1.1 demonstrates the main aspects of literature conducted on the conservation and documentation of the Fatih mosque.

Table 1.1: Comparison Between the Literature Conducted on the Preservation of Fatih Mosque.

Referenced Literature	Year	Focus	Methodology	Findings
(Vatan, 2018)	2018	Assessed the structural system of the domed Fatih mosque.	-Studied construction techniques. -Analyzed past damages records.	Reported structural problems caused by the unsymmetrical old plan and the thin exterior walls.
(Akyuz et al., 2015)	2015	Characterized the type of plaster and mortar used in the wall painting of the Fatih mosque.	Used EDXRF micro-Raman and FTIR analyzing techniques.	Concluded that the plaster mortars belong to the mixed lime–gypsum mortar group.
(Beyen, 2008)	2008	Identified structural problems after the 1999 earthquake.	Utilized a digital converter, DT-2827 A/D board with 16-bit A/D converter at a high speed of 100 kHz accommodating.	Presented graphs and records of structural past, current, and expected behavior.
(Berilgen, 2007)	2007	-Analyzed the local soil condition. -Predicted the site's future behavior for future earthquakes.	Employed horizontal/vertical FAS ratios and bedrock input motion to test future behaviors.	Concluded that the soil played a huge role in the cause of structural damage in past earthquakes.
(Yastıklı & Alkı, 2003)	2003	Documented the existing mosque using close-range photogrammetry.	Took 230 images with a semi-metric Rolleiflex 6008 tool.	Produced a 3D vector and raster data model of Fatih mosque.
(Kunter & Ülgen, 1939)	1939	-Aimed to understand the history of the mosque. -Obtained spiritual evidence and valuable information.	-Evaluated past visual and written records including drawings and manuscripts.	Found valuable information on the mosque's history before and after the old structure collapsed.

Other literature presented information regarding the cost and amount of materials used for the construction of the new structure, however, little information was provided on the

restoration and repair methods (Yayınları, 2013). Despite the mosque's urgent concern for long-term conservation, there is a notable gap in the utilization of advanced technologies and literature on the preservation and documentation of the Fatih mosque. This is due to the loss of its original structure after the earthquake and not focusing on documenting the original historical features in the reconstruction phase. Therefore, this research aims to unravel two dimensions: First, generating a digital point cloud model for two of the Fatih mosque's façades. Second, semantically segmenting the model to extract building elements for future analysis and observations.

By achieving these objectives, the study contributes to:

a. Serving the urgent need for a long-term and sustainable conservation solution.

b. Producing trained data on the Fatih Mosque that can be utilized for the element's segmentation on other mosques with similar architectural features and language.

c. Providing a sharable digital model that serves different professions.

d. Digitalization of data acquisition and building elements' detecting workflow.

To better tackle the digitalization of the Fatih mosque, employing point cloud semantic segmentation for the mosque's analysis and elements extraction offers an innovative solution for tackling the difficulties of conserving such a large and complex structure.

2. POINT CLOUD SEGMENTATION

Digitalizing the documentation and preservation processes of heritage buildings contributes to better decisions regarding their restoration, alteration, renovation, and conservation. With the utilization of point cloud semantic segmentation, each element of the heritage building can be analyzed and shared among different professions. This chapter presents the point cloud data collection, and semantic segmentation techniques, with the role of building elements segmentation for heritage analysis.

2.1 POINT CLOUD DATA COLLECTION TECHNIQUES

Point cloud models consist of a massive number of points that digitally represent the captured building, each point in the model has its properties such as color, reflection and position (Yang et al., 2023). Wang & Kim (2019) defined point cloud models as three-dimensional models with x,y,z coordinates representing surface information such as texture and reflectance. Because of recent technological advancements, multiple tools nowadays can be used for data collection of heritage point cloud models, without relying on traditional methods and direct contact (Feroz & Dabous, 2021). Data collection refers to the act of capturing a building or an object using different tools and equipment like cameras and laser scanners (Moyano, Nieto-Julián, et al., 2021). Moreover, it is the procedure of using technological equipment for capturing and documenting existing buildings (Rashidi et al., 2020). These tools can determine the accuracy and level of detail of the produced model. Therefore, prior planning for the chosen data collection tool is important to avoid data loss and possible errors. Despite which method is used, the captured data represent existing buildings in the form of a digital 3D mesh or a point cloud model that can be virtually accessed for analysis, examination, and measurements (Opoku et al., 2021). As shown in Chart 2.1, point cloud data collection procedures can be carried out using two main tools which are (a) Photogrammetry (Martínez-Carricondo et al., 2021) (Kanun et al., 2021) (Higueras et al., 2021) (Pang & Biljecki, 2022). (b) Laser Scanners (Zou et al., 2021) (Solla et al., 2020). Or the combination of both (Andriasyan et al., 2020) (Mohammadi et al., 2021) (Alshawabkeh et al., 2020) (Alshawabkeh & Baik, 2023).

Chart 2.1: Point Cloud Models Data Collection Tools.

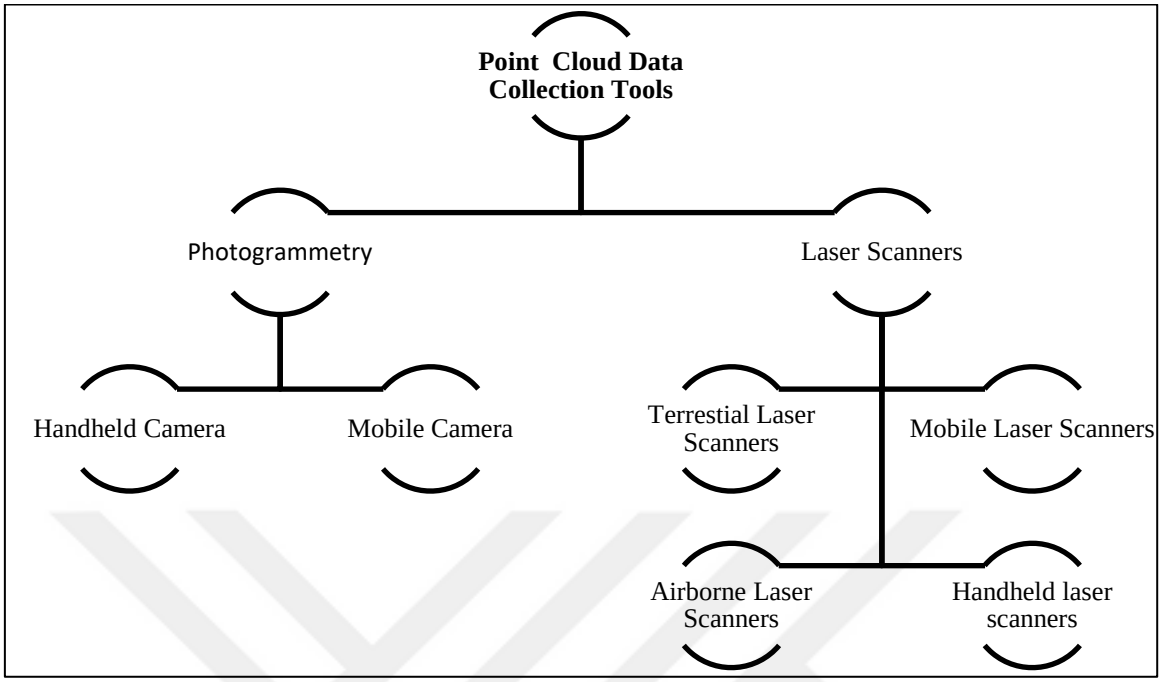

This chart displays the two main equipment used for collecting data from heritage buildings. Several types lie under each main equipment, which are the most used and known types for heritage capturing, however, other types that are not related to the heritage sector are available but are not within the study scope. Both tools are great for use in the AEC (Architecture- Engineering -Construction) industries because of their ability to capture accurate three-dimensional models from real life and turn them into sharable digital models (Kanun et al., 2021). Both methods perform effectively in capturing data from different buildings with various scales, complexity, level of detail, and architectural languages (Mateus et al., 2019). However, the choice of equipment relies on the building's requirements and the digitalization purpose and scope.

A regularly posed question is whether to use laser scanners, photogrammetry, or a combination of both. The selection of a suitable method is affected by multiple aspects such as the data scale, the building's complexity, the documentation purpose, and the user's accessibility to the available equipment. Table 2.1 displays a summary of the difference between the data collection strategies used in literature for heritage digital model acquisition.

Table 2.1: Comparison Between Photogrammetry and Laser Scanners for Data Collection of Heritage Buildings.

Comparison Factors	**Laser Scanners**	**Photogrammetry**
Point's Information	• RGB • Position • Reflectance intensity	• RGB • Position • Textures
Cost	Expensive	Affordable
Flexibility	Limited movability	Flexible
Usage	• Complex use • Require professionals	Ease of use
Limitations	• Affected by material reflectivity	• Affected by shadows • Need for image scaling

Even though both methods produce high-quality digital models, previous studies have established that photogrammetry is starting to replace laser scanners, especially within the architectural field, which focuses mainly on digital documentation rather than developing and prosing new programming-oriented digital heritage studies (Mohammadi et al., 2021) (Yang et al., 2023). This goes back to the photogrammetry approach's ability to replace traditional data collection methods with a cost-effective, flexible, and easy-to-use tool (Koutsoudis et al., 2020). This approach is particularly suitable for experimental architecture like this study done on the Fatih mosque. Which aims to produce a digital heritage model and help establish a solid foundation for a fully automated and low-cost approach for data collection and interpretation of complex heritage buildings with different architectural languages. To better understand the usability of the mentioned tool, each method is explained with examples of its applications.

Laser scanners provide accurate digital representations of heritage buildings by capturing the real structure and turning it into points, where each point has its own characteristics such as its position, color, and reflectance intensity (Mohammadi et al., 2021). The term laser scanner doesn't only imply one instrument, it encompasses different types that serve multiple functions based on the accuracy level, the capturing purpose, and the object's surrounding

environment (Boardman & Bryan, 2018). One important aspect that all lasers depend on is the distance between the captured building object and the used equipment, which differs according to the laser type. These types include Terrestrial Laser Scanners (TLS), Mobile Laser Scanners (MLS), Airborne Laser Scanners (ALS), and handheld laser scanners.

Multiple practices have experimented with the use of these types. Quattrini et al. (2015) conducted a 3D reconstruction study on the Church of Santa Maria at Porto-Novo from the Romanesque period using TLS, to perform a quality assessment on the obtained point cloud model. Moreover, Damięcka-Suchocka et al. (2022) used TLS to create a 3D digital copy of a brick wall structure. The captured data showed good results and allowed them to identify cracks, repaired areas, and moisture from the 3D reconstructed model. Di Filippo et al. (2018) argue that the use of standard laser scanners like TLS can be very time-consuming and limiting for capturing narrow spaces. Therefore, they introduced the use of a wearable mobile laser scanner MLS to capture the interior of a historical building while walking within the place by making it more accessible and time-effective. Moreover, using an airborne laser scanner ALS in combination with aerial photogrammetry, Risbøl et al. (2015) were able to successfully identify and document changes that occurred within the last 50 years in a historical landscape site in Norway. Lou et al. (2022) utilized a handheld laser scanner with a camera to extract details and features from a cave in a historical garden in China. They proposed a method to deal with rockery digitalization and control the raw point cloud model to extract better features. The chosen type showed effective results showing opportunities for future improvements and research.

Among all the mentioned types, TLS is the most used type within the digital heritage model generation sector. Because it showed several good practices and benefits in the protection and observation of heritage monuments (Costa et al., 2016). These benefits include the ability to capture highly detailed and accurate digital replicas of historical buildings (Antón et al., 2018), and the ability to capture an inclusive view of the whole structure (Abbate et al., 2020). However, a major challenge with the use of laser scanners for data acquisition is the data's colors efficiency, because the camera position is not always compatible with the scanner position which leads to misleading data fusion (Dostal & Yamafune, 2018). Moreover, in a study done on the minimum number of geometrical features that can be obtained through TLS, Chaudhry et al. (2021) mentioned the insufficiency faced in the

laser's ability to detect edges and cracks, because of the dense point cloud extractions, the coordinates of points near the edges can be misinterpreted. This issue is known as the mixed pixel effect, where the laser's beam is not properly positioned at the edges which results in points' spatial discontinuities (Alshawabkeh et al., 2021). As Q. Wang et al. (2016) state that avoiding these kinds of problems is hard to implement without the use of other assisting methods. In addition to the technical limitations, the complexity of the laser equipment and the process of capturing heritage buildings using advanced tools is very complicated and takes long periods. Other than the fact that accessing laser equipment is difficult and very expensive (Jovanović et al., 2020), the acquired models need further processing and the help of professionals to obtain a digital heritage point cloud model (Fan et al., 2021) (H. E. Pang & Biljecki, 2022). Because of the earlier mentioned issues, data representation and dimensional measurements using only laser scanners can be imprecise and unreliable in replicating accurate and detailed features. Because of these challenges including the high cost, complex use, inaccessibility, and limited moveability of laser scanners, this study utilized a photogrammetry approach ensuring the digitalization of the heritage Fatih mosque using a cost-effective, accessible, and easy-to-use data collection technique.

Photogrammetry, as highlighted by Mikita et al. (2020) is an affordable and accessible approach used to represent heritage buildings through digital point cloud models. Moreover, it refers to the use of a camera tool to capture data of an existing building, where the produced images can be converted into a point cloud model with information on the surface's materials, textures color, and position (Borg et al., 2020). It is typically suggested for capturing data on buildings and structures with detailed and complex architectural elements (Banfi, 2020). The produced point cloud model is obtained using overlapping multiple images captured from different angles, instead of direct measuring.

Photogrammetry has different types, such as a normal handheld camera, a mobile phone, or a digital camera positioned on a vehicle. Among all of them, the most used photogrammetry-based tool is the Unmanned Aerial Vehicles (UAVs) also known as drones. UAVs are cameras placed on moving vehicles that can be controlled remotely by humans, which provides more flexibility and efficiency for obtaining data (Rashidi & Samali, 2020). UAVs can reach and capture small inaccessible areas that laser scanners cannot access because of the equipment's heavyweight and difficulty of carrying (Themistocleous et al., 2016).

Upon the literature, photogrammetry is considered the most effective and least time-consuming approach for data collection of historical assets (Alshawabkeh & Baik, 2023). It can be used for different reasons like surface inspection, materials evaluation, and overall documentation and preservation (Dorafshan et al., 2019). Chart 2.2 introduces the advantages of utilizing a photogrammetry approach for heritage building capturing.

Chart 2.2: Advantages of the Photogrammetry Data Collection Tool.

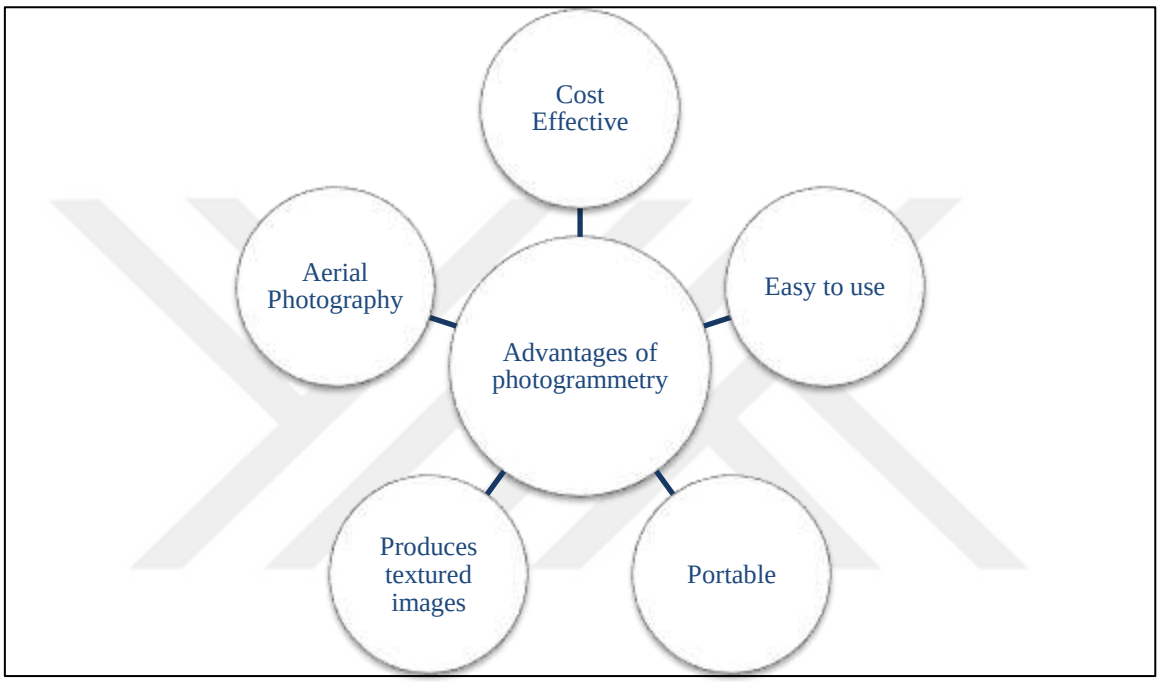

In comparison to laser scanners, it is a cost-effective tool that requires a camera only for capturing (Alidoost & Arefi, 2017). This is particularly effective for budget-constrained projects like this study and other scholarly research. Moreover, it provides high-textured images, showcasing different materials and details of the captured building (Mineo et al., 2022). This is mandatory to perform an accurate semantic segmentation of building elements. The accessibility to photogrammetric tools such as smartphones makes it an ideal and time-effective tool for data collection. It is easy to operate and take to multiple and remote sites. Additionally, it has shown success in the generation point cloud model using data processing software (Alidoost & Arefi, 2017). Among these benefits, a major problem that occurs with a photogrammetry-based approach is the presence of shadows in photos which majorly affects the production of a point cloud model (Arza-García et al., 2019). Moreover, Remondino et al. (2017) stated that the lack of accurate scale and the need for

image scaling and processing is an issue that needs to be further investigated and resolved. These challenges impact the results of the produced point cloud model, which can later affect the segmentation and classification results (Arza-García et al., 2019).

To summarize, both methodologies provide high-quality models that make them suitable for surveying and documenting heritage buildings. However, photogrammetry approaches are more accessible, easier to manage and operate, and more cost-efficient, which motivated this study to implement a photogrammetric approach for the capturing of Fatih mosque in Istanbul. Nonetheless, the captured raw point cloud data has no organized or meaningful structure, representing surfaces without any distinguishable elements highlighted by edges, surfaces, or distinctive geometric features. As Moyano, Nieto-Julián, et al. (2021) declare, the resulting point cloud model from either photogrammetry or laser scanners should be processed and further developed using advanced tools for data processing, cleaning, and semantic segmentation. Therefore, the collected data requires further processing to extract meaningful building elements each with its own properties. This processing can be performed using various ways, one that will be employed for this study is point cloud semantic segmentation.

2.2 POINT CLOUD SEMANTIC SEGMENTATION TECHNIQUES

Point cloud semantic segmentation is crucial for understanding and interpreting 3D replicated point cloud heritage models (Zou et al., 2021). Semantic segmentation is the process of assigning a label to each point in the digital point cloud replica of a real building (Xie et al., 2020). Maru et al. (2023) defined it as the procedure of grouping points with similar characteristics into regions where their properties and features are related. Mostly, old studies experimented with segmentation methodologies using handcrafted features only. These handcrafted features involved human interventions and manual interpretations of each point in the reconstructed model (Zou et al., 2021). Manually labeling each point in heritage digital models is very time-consuming and labor-intensive (J. Zhang et al., 2022). Therefore, Grilli et al. (2017) stated that performing semantic segmentation is crucial to simplify the complexity of point cloud models, by assigning each point to a specific group which helps in obtaining meaningful objects that can be developed into editable 3D models easily. This process focuses on understanding every aspect of each point, from its geometrical structure to the smallest detail of its color and position (Guo et al., 2020).

Most architectural research related to heritage segmentation and preservation focused on very large datasets of heritage benchmarks for testing and training while neglecting other historical landmarks that need to be digitally documented and observed, which is a gap that needs to be addressed in the literature (Zou et al., 2021). This gap led to the realization of the need for more studies focusing on newly captured data from different parts of the world with different scales to explore the digital automation and semi-automation of multiple architectural heritage languages. This motivated this study to be conducted on the Fatih mosque in Istanbul, which is one of the city's most important historical assets. Therefore, employing semantic segmentation for the Fatih mosque's building elements contributes to its preservation, so this heritage treasure can be known by future generations.

With the huge focus on semantic segmentation, various segmentation techniques have emerged. Generally, machine learning and deep learning-based algorithms are used for the classification task for point cloud models. Both techniques perform effectively for the semantic segmentation of heritage 3D models, depending on the type and scale of data. However, the main difference between them lies in how their algorithms function. For segmenting, machine learning applies mathematical algorithms, while deep learning implements artificial neural networks to mimic the human brain and functions (Llamas et al., 2017). Even though machine learning-based algorithms may require some human intervention for data training, their structure has a more straightforward workflow and a faster processing time than deep learning algorithms. On the other hand, deep learning algorithms provide high accuracy of data interpretation but require larger datasets, high computational powers, and someone familiar with programming and the complexity of such algorithms. Given the benefits and challenges of both, the choice of the used technique differs according to the project's type and requirements. To preserve the heritage Fatih mosque using low-cost, fast processing, and easy-to-use techniques, a machine learning approach utilizing the CANUPO classifier was employed.

In machine learning-based methods, a well-known semantic segmentation tool is worth mentioning which is CANUPO. CANUPO is a plugin in the CloudCompare software, used for classifying and labeling point cloud models based on geometric features. Moyano et al. (2021) utilized the CANUPO plugin to classify different building elements from the Casa de Pilatos Palace facade in Seville, Spain. In their study, data was collected using laser scanners.

They performed three segmentation tests, one classified an element from the whole facade, the second focused on the main gate only, and the third emphasized a small retable. The first test showed unsatisfactory results, however, in the second and third tests the algorithm's accuracy increased because the test had smaller point numbers. This highlights the importance of data cleaning methods for point cloud models for the use of the CANUPO plugin. Other techniques include region-growing classification (Nurunnabi et al., 2012), this approach is widely used for grouping points into plane surfaces such as walls and roofs for historical buildings (Paiva et al., 2020), clustering-based segmentation (Galantucci & Fatiguso, 2019), which is suitable for segmenting irregular point clouds, like the detection of surface damage and cracks in heritage buildings (Yang et al., 2023), model fitting (Maltezos & Ioannidis, 2018), this algorithm mainly works with regular point clouds where it detects shapes and geometries and groups points to a relevant category (Li & Shan, 2022), lastly, edge-based classifier, this works by extracting the boundary of points' regions, this machine learning based technique is more effective with the classification of 2D images rather than 3D point clouds (Rabbani et al., 2006).

On the other hand, several studies introduced automated solutions for the detection of building elements utilizing deep learning-based algorithms. Point Net is A widely known framework, a pioneering neural network framework introduced in 2017 by Qi et al, that directly works on unstructured point cloud models. Xiong and Wang (2021) employed PointNet for segmenting elements from an indoor scene. PointNet works by passing points as input data into a series of neural networks, then it groups points with symmetrical features Despite PointNet being a pioneering segmentation technique, Xiong and Wang (2021) state that the classification results showed an overall accuracy of 95%, but it failed at classifying elements with smaller and more complex features. Haznedar et al. (2023), employed PointNet for the segmentation of 28 heritage buildings in Gaziantep, Turkey. Most of the case studies were used as training data, while 20% of them were used for testing. However, PointNet showed unsatisfactory results for the segmentation of these buildings due to the deformation and damage in the condition of the buildings. An improved version of PointNet is the introduction of PointNet++ by Qi et al. (2017), PointNet++ applies the same approach used in PointNet, with the difference of focusing on smaller neighboring points and moving them into bigger groups where the local features can be extracted from. This was performed to extract interior elements like walls, floors, chairs, desks, beds, and doors. It showed

efficient results in its ability to semantically segment points robustly and effectively. Therefore, PointNet++ is more sufficient for its ability to extract features of detailed and complex structures. Another study using a deep learning-based algorithm named DGCNN (Dynamic Graph Convolutional Neural Network) (Pierdicca et al., 2020) aimed at segmenting architectural elements of 11 labels, including columns, arcs, walls, windows, vaults, and roofs. This segmentation technique works by capturing geometrical relationships between neighboring points by changing their order multiple times to learn edge features between them. Other similar studies utilizing deep learning-based approaches are graph-based segmentation. Shen et al. (2018) declare that PointNet has a gap in its ability to recognize fine-grained features within a point's local neighborhood. In response to this gap, Shen et al. (2018) improved the existing framework by introducing a graph-based approach named KCNet. Which employs kernel correlations to define point set kernels. Kernel correlation is the process of extracting similar features and understanding how (kernel points) fit with each other. Then it extracts features from graphs employed on neighboring points. Their experiment focused on segmenting different parts of an object, such as segmenting the chair's seat from its legs, or the table's top from its legs. This technique showed that this algorithm was able to autonomously capture elements, outperforming previous techniques.

The selection of the semantic segmentation technique depends on the availability of tools, the scalability of the data, and the familiarity with the segmentation algorithms. As mentioned above, while DL-based algorithms might provide more accurate results than ML, DL algorithms are more programming-oriented and require professionals to operate, with longer computation time. Therefore, the approach of ML was used, exploring one of its classifiers CANUPO within CloudCompare software. Originally, the plugin was tested on natural scenes like the detection of rock, vegetation, or rivers, while fewer studies implemented it for digital heritage semantic segmentation. Given that the CANUPO classifier wasn't employed on any heritage data captured from Turkey, more specifically heritage data collected using a photogrammetry approach, this methodology applied is original.

2.3 SEMANTIC SEGMENTATION OF BUILDING ELEMENTS

Segmenting building elements serves great benefits within the architectural field, especially for heritage building elements analysis and observation. In the heritage conservation sector, semantic segmentation refers to the interpretation of digital heritage data, by classifying building elements as separate objects that can be developed, analyzed, and imported into engineering software (N. Rocha et al., 2020). It became a widely researched topic with applications used for both 2D images and 3D models. When applied to 3D models, utilizing semantic segmentation is more useful, as it serves as a classification tool that enables the extraction of different building elements that can be shared for analysis and evaluation. This process focuses on isolating and extracting building elements from unstructured and raw digital point cloud data, elements such as walls, windows, doors, columns, and roofs.

Segmenting building elements has been explored intensively for years within different sectors. In the structural engineering field, Hamid-Lakzaeian (2020) experimented with four segmentation techniques applied to three buildings in Dublin, Ireland, to address the issue of segmenting multi-planar façades and differentiating load-bearing elements from the other building elements. The study's results demonstrated an overall accuracy of 91% in the algorithm's ability to distinguish multiple structural elements. Within the urban field, Sun et al. (2024) developed the RandLA-Net algorithm to extract the roof element from the lidar laser scanner data, to solve the complexity of the need for roof reconstruction and restoration. Within the architectural sector, utilizing semantic segmentation supports the automation of heritage building element identification and assessments. Segmenting heritage building elements has various advantages, as seen in Chart 2.3.

Chart 2.3: Role of the Building Elements Semantic Segmentation in Heritage Analysis.

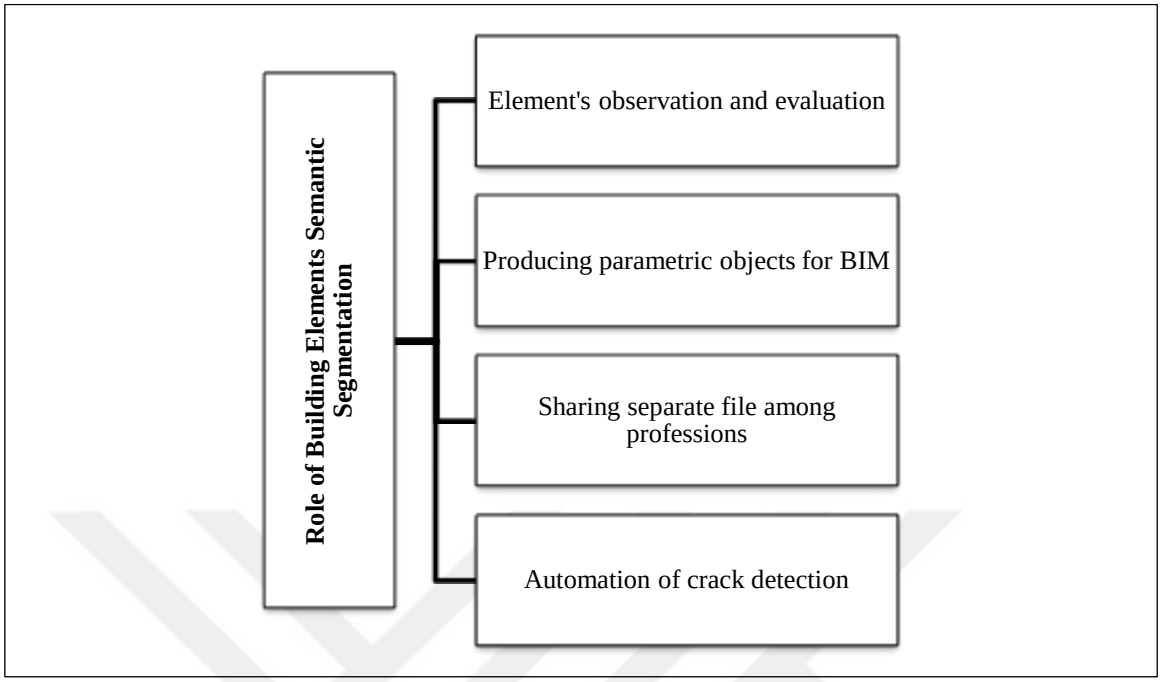

As presented in the chart, segmenting building elements contributes to various aspects within the heritage sector. Conducting a detailed analysis of the heritage building entities was explored by Croce et al. (2021), who utilized an automatic segmentation technique using the CANUPO plugin in CloudCompare software, to label and classify different building elements from the Pisa Charterhouse aiming to transfer the segmented elements into BIM for documentation and observation. Additionally, Malinverni et al. (2019) evaluated the performance of PointNet++, by testing its ability to recognize heritage elements like arcs, columns, walls, and windows performed on both an indoor and outdoor scene from four historical buildings. By using an automated clustering and labeling approach, they aimed at preserving the heritage buildings through the digitalization of these assets, in which the algorithm showed good outcomes that can be further studied and developed. Moyano et al. (2022) applied semantic segmentation to extract structural elements and conduct a detailed structural analysis of the La Anunciación church. Other advantages include simplifying the transformation procedure to BIM software, through the creation of parametric objects that can be shared and edited, done by Macher et al. (2017) the study aimed at extracting structural elements from a historical building, to facilitate its integration within BIM software to provide parametric objects each with its properties within Revit for further analysis and assessments. Similarly, Moyano et al. (2021) used the CANUPO classifier to

identify different architectural elements such as walls, windows, and gates. Using easy-to-operate software without the need for programming or professionals, they moderately succeeded at segmenting some building elements and imported them within BIM software for elements' development and observation. Barrile and Fotia (2021), experimented with the semantic segmentation of a point cloud model of a church capture in Italy using UAVz and laser scanners. They extracted different entities into editable parametric objects. From an accessibility perspective, segmenting building elements enables project sharing and assessment among different professions by providing the targeted elements to each profession separately. Truong-Hong and Lindenbergh (2022) used point cloud segmentation to extract structural components such as concrete walls, columns, and primary and secondary beams from a concrete building, to simplify the structural inspection procedure and distribute the information to their related sector. Likewise, Murtiyoso and Grussenmeyer (2019) explored the use of different geometric-based algorithms to classify historical buildings into multiple elements such as roofs, walls, floors, and structural supports. Particularly, in the second phase they focused on segmenting structural supporting elements like columns and beams. As a result, the algorithms succeeded in classifying the building's elements and further distinguished between columns and Pires. With the aim of preservation, segmenting building elements Supports the automation of damage and crack detection by classifying smaller elements and conducting detailed examinations of them. This facilitates decay and damage detection, which can be applied to different historic structures like castles and monumental buildings as studied by (S. Bruno et al., 2023).

Despite the importance of identifying building elements from the digital heritage model, this process is still rather complex and in need of more research and experimentation. When aiming for heritage elements classification, some challenges might result in wrong segmented points. Moyano et al. (2021) implemented the CANUPO plugin for classifying elements from a palace in Seville, in which the obtained results weren't all satisfactory, because the algorithm failed to classify elements that have the same form but differ in material or colors. This goes back to CANUPO, which mainly performs segmentation based on the shape and form of the captured building elements. Moreover, PointNet, a pioneering segmentation framework that formed the base of many developed segmentation algorithms, still results in inaccurate classification of elements. This was encountered by Xiong and Wang (2021), where the algorithms couldn't classify elements that were in close contact

with each other, like classifying a book on a table, it struggled to distinguish the elements from each other, so it falsely classified the books as part of the table. This indicated that the semantic segmentation field still requires more research experimenting on different buildings using different data managing techniques.

Having outlined the advantages of segmenting building elements for enhanced heritage analysis and interpretation, the following chapter will detail the methodology employed in this study, explaining the workflow and used tools to semantically segment the Fatih mosque's facade elements.

3. METHODOLOGY

The following section describes the workflow used for the digitalization and semantic segmentation of the Fatih mosque building elements. (Figure 3.1) illustrates the utilized methodology in order. However, it is important to highlight that for other studies with the aim of digitalizing and segmentation, the process might differ. The presented steps are not linear, some of them might be skipped, developed, or repeated multiple times. Also, other equipment for the data collection and interpretation may be used.

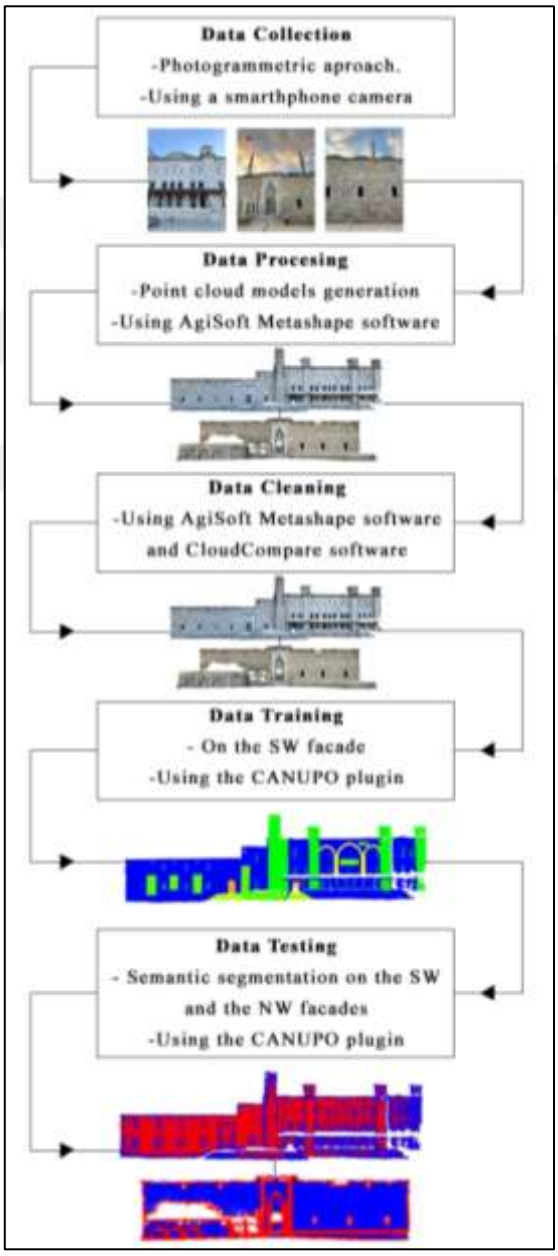

Figure 3.1: Workflow for the Point Cloud Semantic Segmentation of the Fatih Mosque.

The first step is data collection, which requires multiple site visits and equipment to capture the existing historical structure. For this study, photogrammetry was employed using a smartphone camera to capture the southwestern (SW) and northwestern (NW) façades resulting in 261 images from both sides. In the second step, the captured images were processed using Agisoft Metashape Pro software to generate a 3D point cloud model. Agisoft Metshape first generates a sparse point cloud model which the dense point cloud model with more textures and details is built upon. After data processing, data cleaning was applied using manual and automatic techniques, manual techniques were conducted in Agisoft Metashape, while the automatic techniques were utilized within CloudCompare software. Fourth, is data training on the SW side through manual identification of areas representative of the mosque's elements with the utilization of the scale ramp values adjusted based on the targeted element for segmentation. Last comes the classifier testing, by assessing the CANUPO plugin's ability to segment elements from the NW facade, based on the trained data on the SW façade, this gives an insight into the classifier performance and suitability for heritage data.

3.1 DATASET

To apply semantic segmentation, the dataset was divided into two. The first dataset is used for training which is captured from the SW façade. The second dataset is used for testing, and captured from the NW façade. As shown in (Figure 3.2) the red color indicates the longer side of the SW façade which has more elements, and some elements like the windows were repeated which helps the classifier to learn the element's feature better. The green color resembles the shorter side of the NW façade. Two elements from the SW façade weren't in the NW façade, all the façade elements will be explained in the coming chapters.

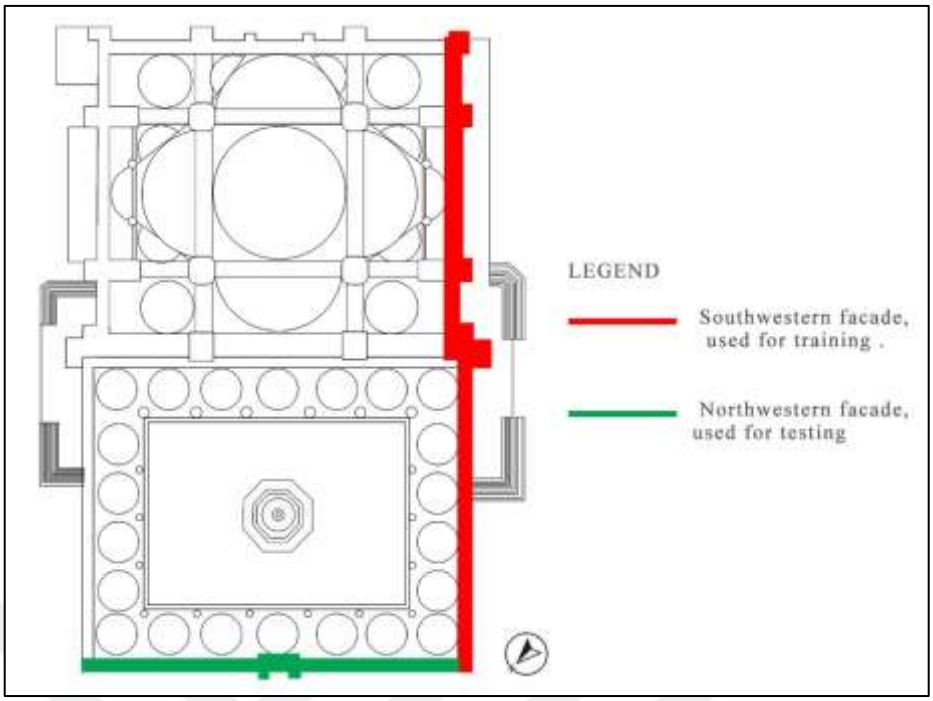

Figure 3.2: The Fatih Mosque's Facades Used for Training and Testing the Semantic Segmentation Classifier.

The other facades, the northeastern and southeastern facades aren't within the study's scope, because both sides couldn't be accessed and captured. Upon multiple visits, the northeastern side was closed for renovation and alteration, covering the whole façade. The southeastern façade can't be accessed in general, because it has a library and the Sultan Mohamed al Fatih's tomb in front of it, which limits its accessibility. However, this limitation doesn't affect the implemented workflow or findings of the study, because both the NE and SE facades have the same elements of this study's data including the SW and NW facades.

This data is relevant for testing and training because the façade elements of the Fatih mosque resemble the Ottoman architectural style, which helps in the digitalization of other mosques with similar elements and features. So, it doesn't only contribute to the preservation of the Fatih mosque but to the digitalization of other buildings with shared characteristics. This dataset helps form the basis of data management procedures. Each one of the captured facades is developed and prepared for segmenting elements. The following chapter introduces the data collection procedure, what was used, and how the NW and SW facades were captured for digitalization and classification.

3.2 FATIH MOSQUE'S DATA COLLECTION AND POINT CLOUD PROCESSING

To prepare the dataset for semantic segmentation, the following steps of data collection using a photogrammetric technique, data processing utilizing Agisoft Metashape, and data cleaning by employing manual and automatic techniques were followed in order.

3.2.1 Data Collection

Regarding the photogrammetry approach's advantages of being cost-effective, accessible, and easy to use, a photogrammetric approach was employed to capture the SW and NW façade of the Fatih mosque. The approach includes using an iPhone 14 Pro Max camera. A smartphone tool is accessible and used by everyone, utilizing such a tool and obtaining good results from it contributes to an accelerated automation of the capturing and documentation process, because it is within the reach of everyone. Multiple visits to the mosque's site were made, to observe the visitor's density, in which crowds affect the capturing procedure resulting in images with non-targeted data such as people, cars, and random objects. Upon observation, most of the visits were at 7 a.m. when little to no people were there which didn't corrupt the capturing workflow. Additionally, at 7 a.m. no harsh sun or visible shadows were present, which contributes to better image and segmentation quality. Another vital aspect was the motion followed when capturing the facades. A steady notion following a horizontal pace was followed to obtain sequential photos of the mosque, to help the classifier in distinguishing the common point between the pictures easier for photos alignment point cloud model generation. Moreover, to capture the broad view of the façade along with some details and ornaments, the images were captured from different distances along both facades, as shown in Table 3.1.

Table 3.1: Sample Images Captured at Different Distances from the Fatih Mosque's SW and NW Facades.

Images Captured from the Southwestern Facade		
Images captured 8 meters away	**Images captured 15 meters away**	**Images captured 20 meters away**
  	  	 
Images captured from the Northwestern Facade		
Images Captured 3 meters away	**Images Captured 8 meters away**	**Images Captured 13 meters away**

Table 3.1: Sample Images Captured at Different Distances from the Fatih Mosque's SW and NW Facades (Table Continued).

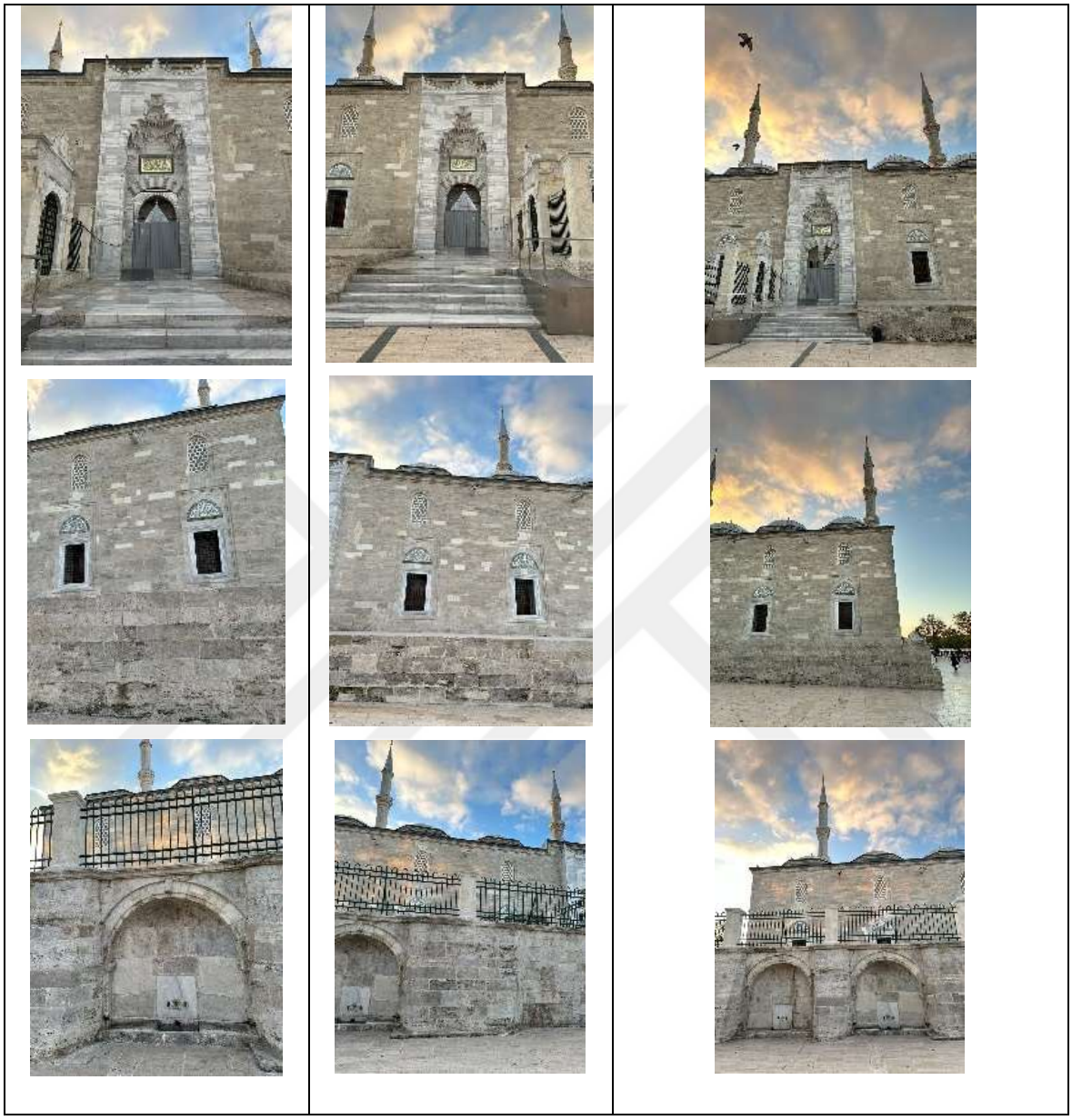

The distances were calculated based on the tiles used in the flooring, which according to the tile size ranged between 60 and 30 cm, the number of tiles was calculated at each distance multiplied by the tile's size resulting in the capturing distance from the targeted façade. The farthest distances from both sides range between 13 to 20 meters away, which covers a broader view of the mosque's elements. The closest distance was 3 to 8 meters away from the facades, this closer range allowed for better capturing of the mosque's ornaments, details, and materials. Collecting data at various distances is crucial to obtain better point cloud

models. For the SW facade, 135 images were captured, while 126 images were taken from the NW façade, resulting in a total of 261 images from both sides. These images were used for data processing and the generation of a digital point cloud model.

3.2.2 Data Processing

To process the 261 images collected from the Fatih mosque's façade, Agisoft Metashape Pro was utilized. Agisoft Metashape founded in 2006, is a photogrammetry processing software (*Agisoft Metashape: Agisoft Metashape*, n.d.). It processes the images carefully by aligning a series of photos taken from various angles and distances, then matching their sharable points known as "tie points" across the images. Tie points are points that are visible in images taken in sequence, which the software detects and connects the imported images according to them. This alignment provides a complete, seamless, and continuous scene or object of the captured data. Once the tie points are distinguished, the software generates an initial sparse point cloud model made from tie points, which doesn't show any visible textures or geometry. The sparse point cloud model can then be turned into a dense point cloud model. This dense model can be exported in different levels of detail, including high, medium, and low resolution, each differing in the number of points it contains. The model's resolution relates to the study's scope and time. Higher resolutions result in more points, details, and clearer textures within the model, and thus a longer processing and interpretation time. To perform semantic segmentation, a dense point cloud model is needed because it offers a clearer representation and a more detailed view of the captured data, which captures finer textures and intricate features.

In this study, data processing started with importing 135 images into Agisoft Metashape Pro, all taken from the SW side. After importing all the images in the program, the align photos function was applied to detect the common tie points across the taken images, by identifying their relative positions and aligning them based on the sequential images that share features between them. The alignment was successful for all 135 images, resulting in an initial sparse point cloud model made from 45,975 tie points which didn't resemble any details or clear geometry of the Fatih mosque's SW facade. Therefore, the build dense cloud feature was used to generate a more textured model that portrays the façade's elements clearly, showcasing the overall SW façade, as illustrated in (Figure 3.3).

Figure 3.3: A 2,267,690 Point Cloud Model of the SW Facade, Captured from Agisoft Metashape.

The dense cloud model generated has 2,267,690 points for the SW façade which provided a rich and detailed representation of the mosque's façade. Almost all of the elements were generated successfully except for elements that are above eye level height like the roof on the right side, along with the flooring, these elements need a a tool to capture the data from a top view. But for the limitation of the photogrammetric approach using a smartphone, elements on higher levels weren't captured and represented. The model was exported in medium resolution, which maintained a manageable dataset size, ideal for this research's aim of capturing larger architectural features instead of smaller ornaments and details. The objective was to represent main elements like masonry walls, main load-bearing walls, columns, and the overall geometry of windows, arches, and entrances. The medium-quality resolution not only minimized the training and testing time on the data but also provided a good and clear representation of the SW side.

For the NW façade, the same methods and processes were applied to obtain the dense point cloud model as shown in (Figure 3.4)

Figure 3.4: A 993,501 Point Cloud Model of the NW Facade, Captured from Agisoft Metashape.

As seen in the figure, partial parts on the left side of the façade weren't correctly represented. This might be because the lower part of the façade is extruded to the outside, where the extruded upper part consisting of balustrades limited the software's ability to replicate the elements behind it, resulting in an empty part within the captured NW façade. The model was exported also in medium quality to have a manageable dataset.

Both digital models served as a foundation tool for CANUPO's plugin semantic segmentation, However, data cleaning techniques were applied to have more controllable and manageable data.

3.2.3 Data Cleaning

For refinement of the generated 3D dense point cloud models, data cleaning methods were implemented using a combination of techniques within Agisoft Metashape Pro and CloudCompare software. CloudCompare, a free and open-source tool for mesh and 3D point cloud processing, is widely used in model cleaning, classification, visualization, and measurement (Girardeau-Montaut, n.d.). CloudCompare has various plugins that serve diverse functions, including CANUPO, which was employed for the semantic segmentation of raw point cloud models of the Fatih mosque's facades. Additionally, the Raster plugin can convert points into raster grids for creating digital elevation, and the contour plugin generates contour lines based on elevation data within the point cloud. CloudCompare's versatility and ease of use make it accessible even to users without programming expertise, and its compatibility with both data collection tools improves its utility.

Initially, the cleaning process started with manual cleaning in Agisoft Metashape, followed by automated techniques in CloudCompare using the Statistical Outlier Removal (SOR) filter and subsampling feature. For the southwest (SW) façade, a manual cleaning process was conducted first in Agisoft using the rectangular selection tool to remove irrelevant points, such as those representing the sky, people, or uncompleted parts of the facade, which don't contribute to the study's dataset. After manual cleaning, the model was exported from Agisoft Metashape in .las format for additional cleaning in CloudCompare.

In CloudCompare, the statistical outlier removal SOR filter was applied as the second cleaning method. This filter distinguishes noise by calculating the average distance between each point and its neighbors, removing points that are very far from this average distance.

Before applying the SOR filter, the initial SW model contained 2,615,530 points, after applying the SOR filter, the number of points was reduced to 2,520,140 points without losing any essential detail of the façade. Finally, the subsampling feature in CloudCompare was employed, and the subsampling feature reduces the number of points based on a set distance or percentage. In this research, a small subsampling ratio of 0.01 m was used to minimize points number while retaining the model's overall structure and details. After subsampling, the SW façade model was reduced further to 2,267,690 points, producing a managable yet clear digital representation model.

For the northwest (NW) façade, only manual cleaning within Agisoft Metashape was performed. This approach was taken due to the lower number of points in this model, which totaled less than one million. Although CloudCompare's cleaning methods significantly reduce processing time, applying multiple data cleaning techniques on a smaller model with fewer points could compromise representation quality and segmentation results. When the SOR filter and subsampling were used on the NW façade, the point count dropped from 993,501 to 570,498 resulting in a loss of nearly half the points, which could impact the model's structural accuracy for classification purposes.

To summarize, the dense point cloud model of the SW façade initially contained 2,615,530 points, reduced to 2,267,690 points after applying three cleaning techniques, a manual one, and two automatic techniques, with a total reduction of 347,840 points. Conversely, the NW façade's dense model began with 998,872 points, reducing only slightly to 993,501 points through manual cleaning alone to preserve its structure and not to compromise on details and geometries. These data-cleaning steps not only optimize large datasets but also facilitate an efficient training and classification process by producing a manageable model that maintains accuracy without unnecessary points.

3.2.4 Ontological Typology of the Fatih Mosque Façade Elements

To document and analyze the architectural details of the Fatih Mosque's Southwest (SW) and Northwest (NW) facades, an ontology was developed that categorizes each façade element. This ontology is adapted and refined from an existing reference (Stouffs & Tunçer, 2015), which introduced the mosque's physical and conceptual elements within the historical context of the Ottoman era. Through this adaptation, the ontology was developed and ajusted

according to the Fatih Mosque, providing details of each main element to reflect its unique architectural characteristics and entities. (Figure 3.5) illustrates the mosque's external facade elements, showing the individual components of each façade element with additional levels of classification.

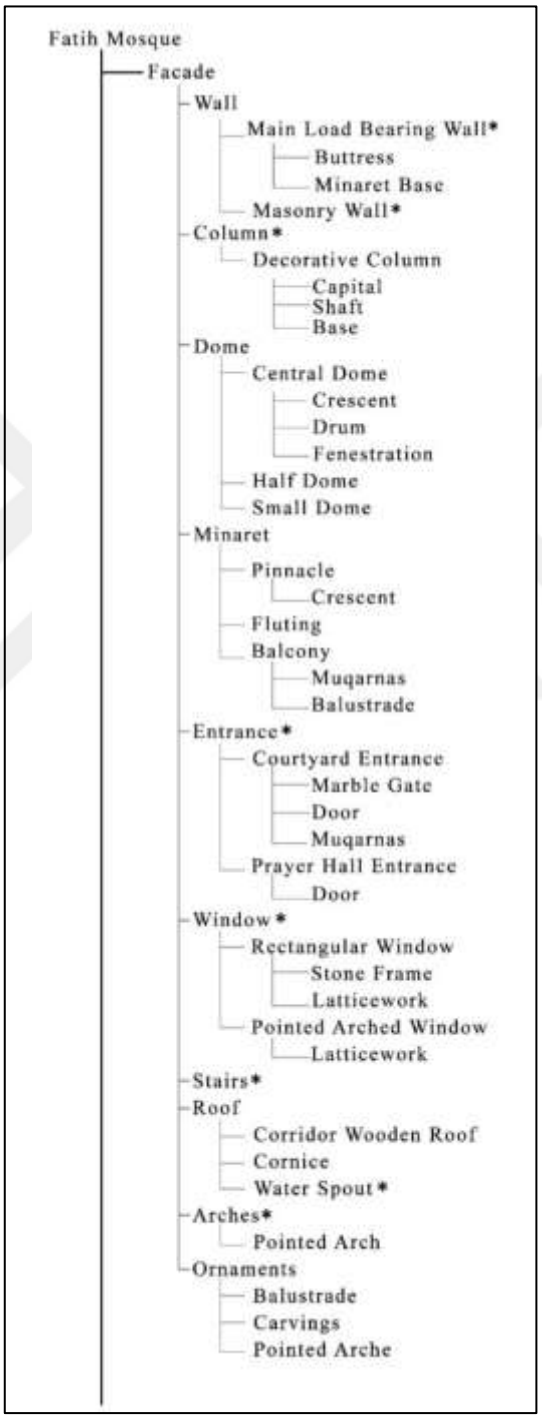

Figure 3.5: An Ontology for the Fatih Mosque's Facade Elements. Elements Marked with an Asterisk (*) are Used for Training and Semantic Segmentation.

This study aims to digitally preserve the Fatih Mosque by extracting and categorizing its primary architectural elements, which led to the identification of eight distinct categories. Rather than selecting categories based on decorative or minor details, the focus remained on major architectural elements, such as main load-bearing walls, masonry walls, columns, entrances, windows, stairs, arches, and waterspouts. For some elements, including the domes and minarets, were excluded due to the limitations of the smartphone-based data collection, which only captured scenes at ground level, omitting complete views of these higher structures.

Additionally, the minaret base required specific categorization, given that only the base was visible within the ground-level data. To address this, the minaret base was classified as a sub-element within the main load bearing wall category, as it shares similar foundational characteristics with buttresses, in which both serve as load-bearing elements attached to masonry walls. In contrast, waterspouts were included as a primary category despite being sub-elements, due to their prominent size and visibility within the façade, in which the classifier detected it multiple times in the segmentation of other elements.

Utilizing these defined categories, semantic segmentation was conducted using the CANUPO plugin in CloudCompare, enabling detailed segmentation of each selected element. This approach offers a structured and replicable framework for analyzing and preserving the architectural heritage of the Fatih Mosque.

3.3 SEMANTIC SEGMENTATION USING CANUPO PLUGIN

Following data cleaning and the identification of architectural elements, the CANUPO plugin was applied for the semantic segmentation of the heritage point cloud model of the Fatih Mosque's Southwest (SW) and Northwest (NW) facades. CANUPO, which stands for *CAractéristiques NUmeriques POintées* in French, is a CloudCompare plugin that supports the classification and analysis of point cloud data through a multi-scale approach (Brodu & Lague, 2012). This plugin uses a scale-based dimensionality criterion to analyze point cloud geometries, distributing core points throughout the model and assessing patterns around each core point based on parameters set along a "scale ramp." The scale ramp includes a minimum (min), maximum (max), and incremental step value to define the range for analysis, where the min and max values determine the smallest and largest distance for analysis around each

point, and the step value indicates the increments between them. By examining clusters, irregularities, and flat surfaces within these ranges, CANUPO enables pattern recognition and ultimately classifies data, albeit through binary segmentation, dividing points into two categories, such as walls and windows or window frame and glass.

To use CANUPO, the classification process unfolds in two main phases: training the classifier and performing the actual classification. During the training phase, sample areas representing each architectural element are manually selected, and the main point cloud model is divided into separate point clouds for each element class. The “train classifier” command is then applied, where two classes, such as walls and windows (class 1 and class 2), are chosen and analyzed based on scale ramp parameters. This analysis results in a classifier file in .prm format, which is used in the second phase to apply the trained classification to the entire model.

In this study, the classifier training phase was initially conducted on the SW facade. This process began with the manual selection of sample areas for each architectural element, as presented before in (Figure 3.5). Using CloudCompare’s segmentation tool, sample areas were isolated by drawing polylines around each identified region as illustrated in (Figure 3.6).

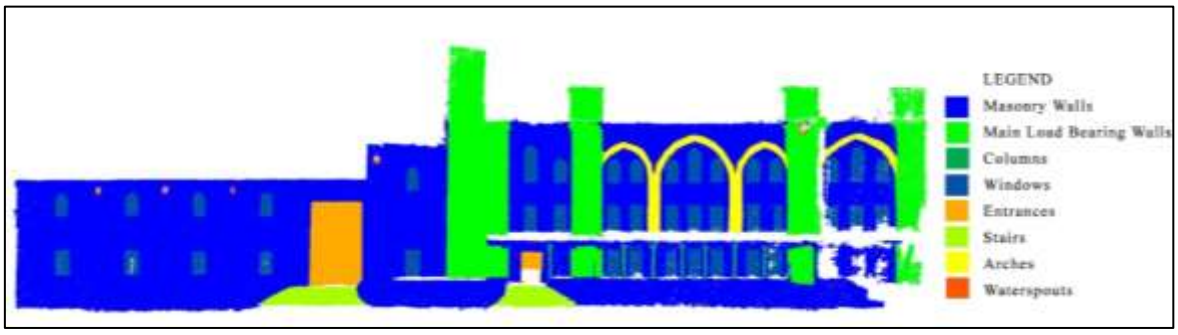

Figure 3.6: Manually Selected Sample Areas Representing the Fatih Mosque’s Facade Elements.

After identifying these areas, each sample was exported as a separate class using the “split cloud according to integer values” command from the scalar field menu. This resulted in multiple point clouds named as integer-based classes (e.g., “class 1” for masonry walls, “class 2” for windows), and a total of eight classes were created from the SW façade, each representing a different architectural element used for training.

Next, CANUPO's "train classifier" feature was employed. Each training session involved pairing a constant "class 1" which is the nontargeted element (the complete façade), and "class 2" the targeted element for classification such as masonry walls, columns, or stairs. To achieve optimal training and segmentation of the training data, the scale ramp values were changed nine to 9 times for the training of each element. In these trials, two of the three scale ramp values min, max, and step were kept constant while changing the third one, producing nine classifier files per facade element, after conducting three experiments for each value. After each changing the scale ramp parameters, the "CANUPO training" windows appear as shown in (Figure 3.7).

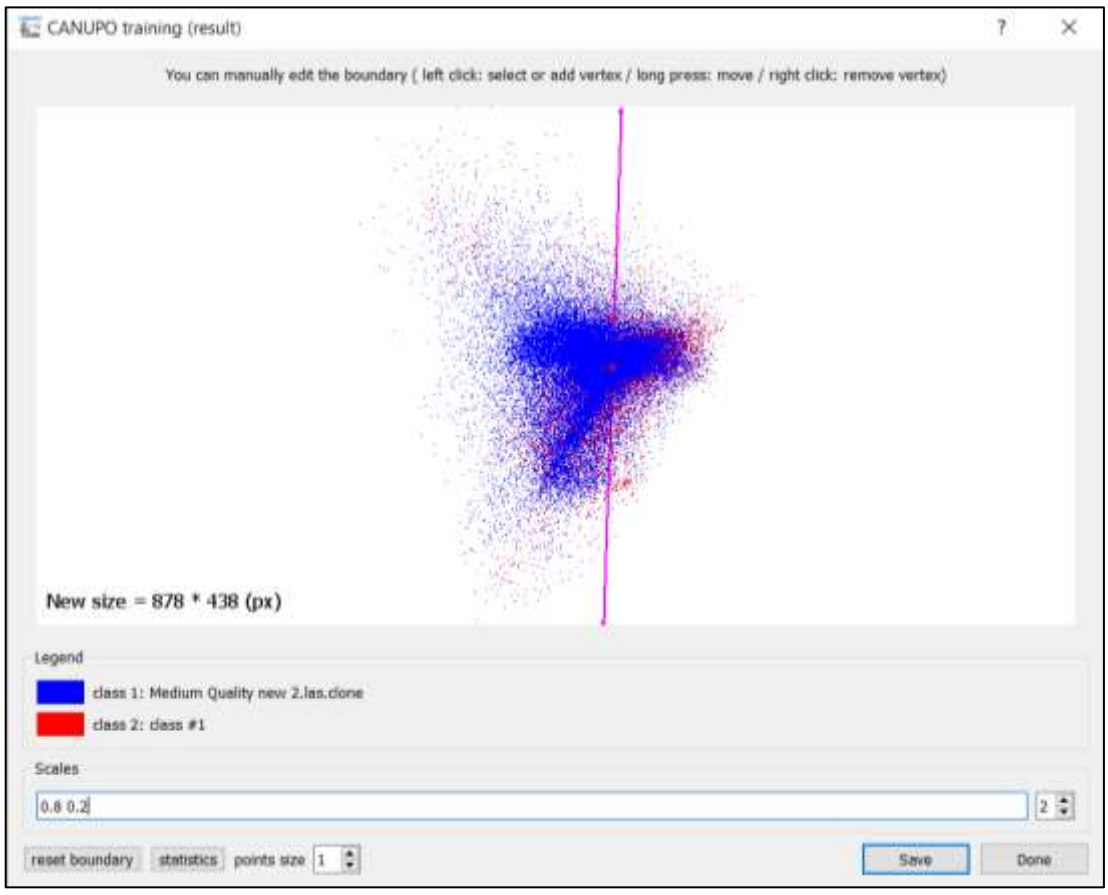

Figure 3.7: CANUPO's Training Window Result Based on the Set Scale Ramp Values, Obtained from the Training for Windows Class.

This window displays how CANUPO categorizes the points according to the scale ramp value. Where the purple line represents the boundary line that separates class 1 in blue

(nontargeted element) and class 2 in red (targeted element), which is determined by the CANUPO algorithm based on the set scale ramp parameters and based on the distance it analyzed between each point and its neighbors. The "Scales" field at the bottom, with values like "0.8 0.2," indicates the minimum and maximum scales used for classifying points based on their neighborhood characteristics, influencing how sensitive the classification is to variations in the point cloud. The boundary line can be manually adjusted and moved to separate the classes more accurately. After managing this process, the classifier file is produced. Ultimately, these classifier files were applied to classify the mosque's elements, on the training dataset from the SW facade, Table 3.2 displays samples of the results obtained based on changing the scale ramp values for each element. For the complete results explored on all eight elements, please refer to Table A.1 in the appendix section.

Table 3.2: Samples from CANUPO's Training Trails on the SW Facade, Based on Changing the Scale Ramp Min, Max, and Step Values. Only Scale Values Marked with an Asterisk (*) Symbol were Used for Testing.

Class	Value	Segmentation Results		
Windows	Max	Min: 0.2, Step: 0.4, Max: 0.6 	Min: 0.2, Step: 0.4, Max:0.8 * 	Min: 0.2, Step: 0.4, Max: 1.0 
	Step	Min: 0.2, Step: 0.3, Max: 0.8 	Min: 0.2, Step: 0.4, Max: 0.8 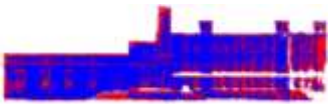	Min: 0.2, Step: 0.6, Max: 0.8 
	Min	Min:0.08, Step: 0.4, Max: 0.8 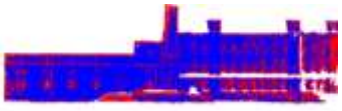	Min: 0.2, Step: 0.4, Max: 0.8 	Min: 0.3, Step:0., Max: 0.8 
		Min:0.2, Step: 0.4, Max: 0.6	Min: 0.2, Step: 0.4, Max: 0.8	Min: 0.2, Step: 0.4, Max: 1.0

Table 3.2: Samples from CANUPO's Training Trails on the SW Facade, Based on Changing the Scale Ramp Min, Max, and Step Values. Only Scale Values Marked with an Asterisk (*) Symbol were Used for Testing. (Table Continued)

			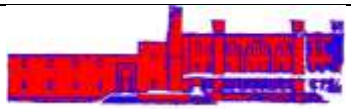	
	Step	Min: 0.2, Step: 0.3, Max: 0.8 	Min: 0.2, Step: 0.4, Max: 0.8 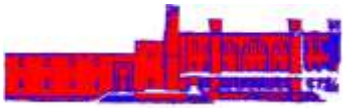	Min: 0.2, Step: 0.6, Max:0.8 
	Min	Min: 0.08, Step:0.6, Max: 0.8 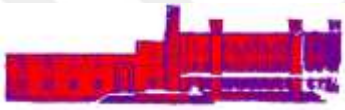	Min: 0.2, Step: 0.6, Max: 0.8 * 	Min: 0.4, Step: 0.6, Max: 0.8 
Columns	**Max**	Min: 0.2, Step: 0.6, Max: 1.0 	Min: 0.2, Step: 0.6, Max: 0.8 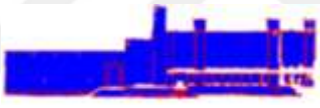	Min: 0.2, Step: 0.6, Max: 1.2 * 
	Step	Min: 0.2, Step: 0.6, Max: 1.2 	Min: 0.2, Step: 0.8, 1.2 	Min: 0.2, Step: 1.0, Max: 1.2 
	Min	Min: 0.2, Step: 0.8, Max: 1.2 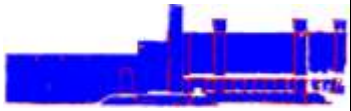	Min: 0.4, Step: 0.8, Max: 1.2 	Min: 0.6, Step: 0.8, Max: 1.2 

The mentioned number in the tables represents the scale value parameters, in which numbers like 0.2 or 1.2 are in meters, these are the min and max values the classifier will analyze. Based on the obtained results, one segmentation outcome for each element was chosen, which is the best result where the classifier performed well in identifying the trained and

targeted element. The chosen scale ramp value was saved into a .prm classifier file. This file was utilized later to test CANUPO's ability to detect the same element using parameters based on the trained data from the SW side, to test its functionality in recognizing it from unfamiliar data of the NW facade. Table 3.3 outlines the results of the testing phase applied to the NW facade using classifiers trained from the SW side.

Table 3.3: Semantic Segmentation Results on the NW Dataset Used for Testing CANUPO's Functionality for Heritage Data.

Class	**Segmentation Results**
Windows	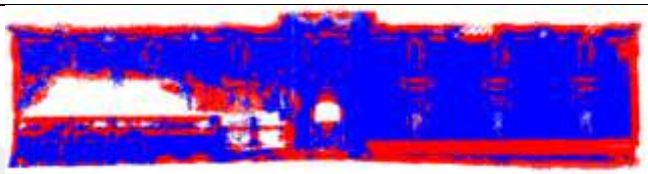
Masonry Walls	
Stairs	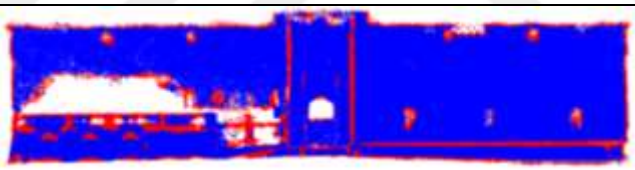
Entrance	
Arches	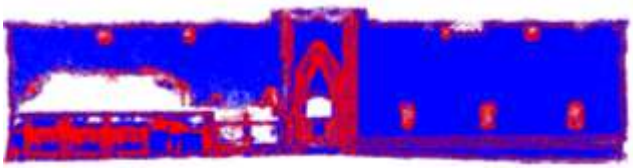
Waterspouts	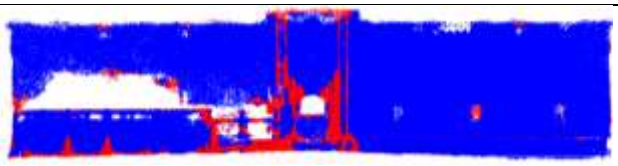

The training phase required a lot of repetition and adjustments to obtain the classifier file with the most accuracy, however, the testing phase was significantly shorter in time because it didn't require any experimentation with the scale ramp values, using the classifier files from the SW facades, each segmentation results on the NW side was acquired within seconds.

Even though CANUPO's performance can be quite distinguished visually from the segmentation result on both facades, reliable assessment criteria were applied to calculate scientifically how many points were correctly and incorrectly classified. Because depending on visual interpretation is subjective, with a lack of actual data on the resulting numbers. Therefore, the segmentation trials presented in Table 4, Table 4A, and Table 5 in the appendix section formed the basis of the next chapter on the assessment of CANUPO's performance.

3.4 ASSESSMENT OF THE CANUPO'S CLASSIFIER PERFORMANCE

To evaluate the results generated by the CANUPO plugin, classification metrics including accuracy, recall, precision, and false positive rate (FPR), were used to assess its effectiveness in identifying the elements on the Fatih Mosque's facade. This method provides a robust measure of the plugin's performance in accurately detecting the facade components and allows for an overall understanding of the classifier's capabilities.

3.4.1 Confusion Matrix Points

Before the calculation of the confusion matrix points, the identification of Ground Truth Points is essential which forms the base of the assessment criteria. To establish ground truth points (GTP), previously illustrated manually selected areas in Figure 11 were used as a baseline. These representative points were carefully chosen to optimally reflect the various elements, ensuring accuracy in the classification of each component. After identifying the GTP for each element, the specific counts for these points were recorded.

In machine learning classification, after the identification of GTP, the segmentation results are analyzed through a confusion matrix, which categorizes four types of points: True Positive (TP), True Negative (TN), False Positive (FP), and False Negative (FN).

a. True Positives (TP) represent points that belong to the segmented class and were accurately classified.

b. False Positives (FP) are points that do not belong to the class but were incorrectly classified as positive.

c. False Negatives (FN) are points that belong to the class but were mistakenly classified as negative.

d. True Negatives (TN) are points that do not belong to the class and were correctly classified.

Following GTP identification, the TP points were identified. Since CANUPO performs binary classification, each segmentation separates the targeted element from the general facade. Using the "split cloud by integer values" command, each class could be individually analyzed, resulting in TP and FP points for the targeted element. TP points were obtained by manually selecting the representative areas corresponding to the GTP. FP points were calculated using equation 3.1

$$FP = Total\ Number\ of\ Points\ from\ the\ Targeted\ Element - TP \quad (3.1)$$

The other binary class, the facade, consists of FN and TN points. To determine FN points, equation 3.2 was used, since manually identified GTP includes both TP and FN

$$FN = GTP - TP \quad (3.2)$$

Lastly, TN was derived by subtracting FN from the total points in the facade, as shown in equation 3.3

$$TN = Total\ Number\ of\ the\ Facade's\ Points - FN \quad (3.3)$$

Using these formulas in combination with manual identification, the GTP, TP, FP, TN, and FN points were calculated. Table 3.4 displays the confusion matrix point numbers according to each segmented facade element.

Table 3.4: Number of GTP, and Points within the Confusion Matrix Including TP, FP, TN, and FN Points Based on Each Element's Segmentation Result.

Segmented Class	GTP	TP Points	FP Points	TN Points	FN Points
Southwestern Façade					
Masonry Walls	1,280,605	726,995	537,633	553,610	449,452
Main Load Bearing Walls	548,764	211,239	216,848	337,525	1,502,078
Columns	19,817	19,228	235,219	589	2,012,654
Windows	200,196	167,042	605,421	33,154	1,462,073
Entrances	75,617	50,691	652,435	24,926	1,539,638
Stairs	88,106	77,501	443,172	10,605	1,736,412
Arches	47,442	35,346	581,765	12,096	1,638,483
Waterspouts	7,143	7,023	198,526	120	2,062,021
Northwestern Facade					
Masonry Walls	811,469	626,873	99,905	184,596	82,127
Windows	41,698	22,888	290,299	18,810	661,504
Entrances	118,610	91,736	304,246	26,874	570,645
Stairs	14,749	5,462	183,565	9,287	795,587
Arches	5,409	5,328	276,629	81	711,463
Waterspouts	1,575	0	115701	1,575	876,225

These resulting confusion matrix numbers for each class were used for the evaluation metrics formulas, which provide a detailed insight into the classifier's performance and help to understand what each number contributes to, and what can be developed based on them. The following section introduces the formulas used for CANUPO's evaluation.

3.4.2 Evaluation Assessment Matrices

To quantify the classifier's accuracy, recall, precision, and FPR for each element, equations (3.4), (3.5), (3.6), and (3.7), derived from Macher, Landes, & Grussenmeyer (2017), were applied:

To calculate the accuracy percentage per class equation 3.4 was used. Accuracy calculates the overall performance of the classifier, as it evaluates its ability to correctly detect the positive and negative points. Using this equation the accuracy percentage was obtained.

$$Accuracy = \frac{TP + TN}{TP + TN + FP + FN} \times 100\% \tag{3.4}$$

While recall (True Positives rate), is calculated to evaluate the number of positive points that were correctly classified by CANUPO. Using equation 3.5 the recall was calculated.

$$Recall = \frac{TP}{TP + FN} \times 100\% \tag{3.5}$$

The precision metric shows how many points were predicted to be positive, but they were actually positive, it tests how accurate the correct classifications are. Using equation 3.6 precision was calculated.

$$Precision = \frac{TP}{TP + FP} \times 100\% \tag{3.6}$$

Lastly, the False Positives Rate FPR, calculates the proportion of actual negatives incorrectly classified within the positives segmented element. Using equation 3.7 the FPR was calculated.

$$False\ Positive\ Rate = \frac{FP}{FP + TN} \times 100\% \tag{3.7}$$

Measuring these metrics gives a clear view of CANUPO's accuracy performance, completeness, precision, and minimization of false classification. According to the obtained

percentages from each metric for each class, ranges including high, medium, and low were set. Percentages with a percentage above 75% are considered high, while percentages from 50 to 75% are considered medium, and percentages below 50% are considered low, where half of the points are incorrectly classified. However, some limitations should be addressed for the interpretation of these results. First, because the identification of GTP and TP points was manually conducted, some points might be falsely identified because it is subjected to human error and intervention. After all, the dataset is big and hard to manage manually with complete accuracy. About this limitation, the representative areas were selected as accurately as possible. Second, because the NW facade wasn't originally used for training, manual identification of its representative areas was conducted to obtain the evaluation assessment metrics. Because comparing its results with the points of the SW facade won't be reliable and accurate. Third, for the masonry walls class, the GTP and TP points numbers don't specifically represent the walls' true points number only. It consists of other facade elements like the ornamental carvings and stones above the windows which aren't targeted for segmentation because this research focuses on segmenting the main façade elements rather than its ornaments and details. However, because the classifier was trained with the same consideration of having the ornament within the masonry wall representative areas, this didn't affect the CANUPO classifier's performance or the way it was evaluated. The following chapter presents segmentation results based on the evaluation metrics criteria with percentages identifying the classifier's effectiveness.

4. RESULTS

This chapter introduces the findings from the CANUPO's classifier performance. In the first phase, the classifier was trained to extract eight building elements from the SW faced. In the second phase, the classifier was tested on its ability to detect the same elements but from unseen data of the NW facade. Based on these phases, the segmentation results were acquired, observed, and analyzed. Table 3.4 displays the outcome of the analysis procedure, which revolved around the calculation of the assessment evaluation percentages, as displayed in Table 4.1.

Table 4.1: Accuracy, Recall, Precision, and FPR Percentages for the Segmented Classes.

Targeted Class	Accuracy Percentage	Recall Percentage	Precision Percentage	False Positive Rate Percentage
Southwestern Façade				
Masonry Walls	52%	57%	57%	54%
Main Load Bearing Walls	76%	38%	49%	13%
Columns	90%	97%	8%	10%
Windows	72%	83%	22%	29%
Entrances	70%	67%	7%	30%
Stairs	80%	88%	15%	20%
Arches	74%	75%	6%	26%
Waterspouts	91%	98%	3%	9%
Northwestern Façade				
Masonry Walls	71%	77%	86%	55%
Windows	69%	55%	7%	30%
Entrances	67%	77%	23%	35%
Stairs	81%	37%	3%	19%
Arches	72%	99%	2%	28%
Waterspouts	88%	0%	0%	12%

For a better and more concise analysis of the results in Table 7, the evaluation assessment percentages of each element are presented below and categorized according to each façade. The resulting percentages are assigned within the high, medium, and low range, provided with an explanation of each number and range.

a. Southwestern Façade Evaluation Metrics

Masonry Walls Class

a. Accuracy: 52% (Medium)

b. Recall: 57% (Medium)

c. Precision: 57% (Medium)

d. FPR: 54% (Medium)

The classification of masonry walls displayed a moderate level of performance across all metrics. While the segmentation results clearly distinguish masonry walls from other facade elements, the medium recall and precision reveal that the classifier struggled to identify a significant portion of true positive (TP) points, missing nearly half of the correct data. Additionally, the false positive rate (FPR) of 54% highlights a decent rate of misclassification, with nearly half of the points incorrectly assigned to this class. This outcome emphasizes the challenges faced by the classifier in effectively differentiating masonry walls from non-targeted elements.

Main Load-Bearing Walls Class

a. Accuracy: 76% (High)

b. Recall: 38% (Low)

c. Precision: 49% (Low)

d. FPR: 13% (Low)

Despite the high accuracy of 76%, the low recall and precision percentages indicate that the classifier struggled to detect many true positive points, misidentifying approximately half of the predicted points. As seen in (Figure 4.1) this performance highlights the classifier's limited effectiveness in isolating the specific geometry of load-bearing walls.

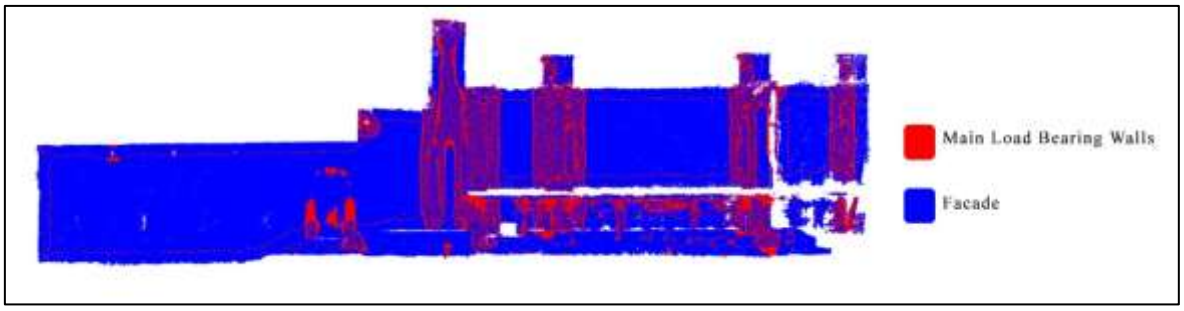

Figure 4.1: Segmentation Result of the Main Load Bearing Walls from the Trained Dataset on the SW Facade.

The higher accuracy can be attributed to the low FPR of 13%, which indicates fewer errors in classifying non-targeted elements.

Columns Class

a. Accuracy: 90% (High)

b. Recall: 97% (High)

c. Precision: 8% (Low)

d. FPR: 10% (Low)

The classifier performed well in identifying the majority of the column's points, as can be seen visually in (Figure 4.2) and numerically by the high accuracy and recall scores of 90 and 97%. However, the low precision suggests significant confusion, with many non-column points incorrectly classified as part of this element. This misclassification likely stems from the geometric similarities between columns and other vertical facade features, requiring more refined parameter adjustments to improve differentiation.

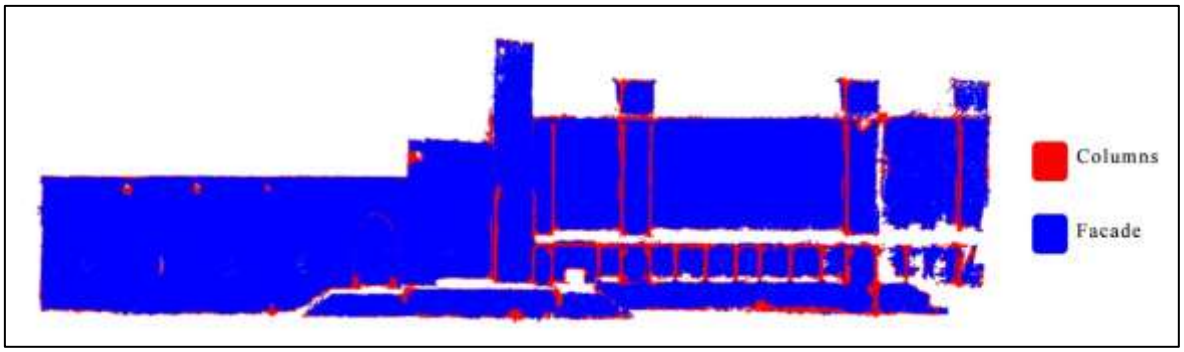

Figure 4.2: Segmentation Result of the Columns' Class from the Trained Dataset on the SW Facade.

Windows Class

a. Accuracy: 72% (Medium)

b. Recall: 83% (High)

c. Precision: 22% (Low)

d. FPR: 29% (Low)

The segmentation of windows demonstrated moderate accuracy and high recall, indicating the classifier's effectiveness in identifying a portion of true positive points. However, the precision score of 22% illustrated frequent misclassification, where a significant number of non-window points were falsely assigned within the windows class. These errors were likely influenced by the intricate details and varied shapes of the windows.

Entrances Class

a. Accuracy: 70% (Medium)

b. Recall: 67% (Medium)

c. Precision: 7% (Low)

d. FPR: 30% (Low)

The performance for entrances was moderately effective, as indicated by the medium accuracy and recall scores. The relatively distinct geometry of entrances, along with their material composition, likely contributed to the classifier's low FPR of 30%. However, the low precision of 7% suggests frequent misclassification of unrelated elements, highlighting a need for improved parameter tuning.

Stairs Class

a. Accuracy: 80% (High)

b. Recall: 88% (High)

c. Precision: 15% (Low)

d. FPR: 20% (Low)

The classifier achieved strong accuracy and recall scores for stairs, indicating effective detection of true positive points. However, the precision score of 15% points to significant

confusion, with many incorrectly classified points. This differentiation in percentages suggests that while the classifier could locate the general shape of stairs, its ability to isolate them from the facade's other geometric features remains limited.

Arches Class

a. Accuracy: 74% (Medium)

b. Recall: 75% (Medium)

c. Precision: 6% (Low)

d. FPR: 26% (Low)

The moderate accuracy and recall scores highlight the classifier’s ability to recognize arches but with limited precision. The low precision of 6% indicates confusion between arches and other curved elements, such as entrances and pointed arch windows. This overlap suggests that curvature alone is insufficient for accurate classification, necessitating additional distinguishing parameters.

Waterspouts Class

a. Accuracy: 91% (High)

b. Recall: 98% (High)

c. Precision: 3% (Low)

d. FPR: 9% (Low)

The classification of waterspouts demonstrated the highest accuracy and recall percentages among all the elements, confirming that the classifier effectively detected most of the true positive points. However, the low precision indicates significant confusion, with numerous false positive points misclassified as waterspouts. This is likely due to the small size and repetitive nature of waterspouts, which may be visually similar to other facade features.

b. Northwestern Facade Evaluation Metrics

Masonry Walls Class

a. Accuracy: 71% (Medium)

b. Recall: 77% (High)

c. Precision: 86% (High)

d. FPR: 55% (Medium)

On the unseen NW facade, the classifier achieved high recall and precision, indicating effective detection of true positive points. Even though the masonry walls can be easily distinguished visually as seen in (Figure 4.3) the FPR of 55% highlights significant misclassification of non-targeted elements, such as upper windows and entrance features. This outcome underscores the classifier's limited generalizability in distinguishing masonry walls when applied to new datasets.

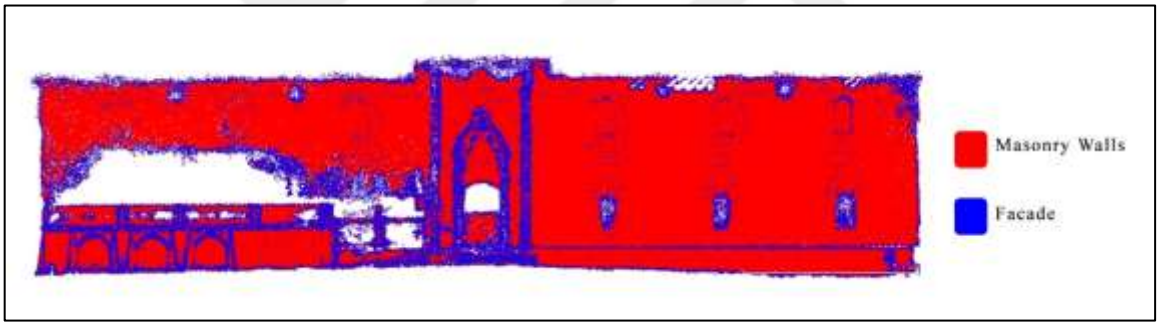

Figure 4.3: Segmentation Result of the Masonry Walls Class from the Testing Dataset on the NW Facade.

Windows Class

a. Accuracy: 69% (Medium)

b. Recall: 55% (Medium)

c. Precision: 7% (Low)

d. FPR: 30% (Low)

The classifier demonstrated moderate performance in segmenting windows, with a recall of 55% indicating partial success in detecting true positive points. However, the low precision

and FPR percentages reveal substantial difficulty in distinguishing window geometry, particularly for upper-level windows, when applied to unseen data.

Entrances Class

a. Accuracy: 67% (Medium)
b. Recall: 77% (High)
c. Precision: 23% (Low)
d. FPR: 35% (Low)

The classifier's medium accuracy and high recall for entrances suggest that it successfully identified a large portion of true positive points. However, the low precision points to confusion with similarly curved features, such as arches and pointed windows, which highlights a need for further refinement.

Stairs Class

a. Accuracy: 81% (High)
b. Recall: 37% (Low)
c. Precision: 3% (Low)
d. FPR: 19% (Low)

While the classifier achieved high accuracy for stairs, the low recall and precision scores reflect its struggle to correctly classify stair elements. The high accuracy was primarily influenced by the low FPR, indicating fewer mistakes in misclassifying non-targeted points.

Arches Class

a. Accuracy: 72% (Medium)
b. Recall: 99% (High)
c. Precision: 2% (Low)
d. FPR: 28% (Low)

The classifier demonstrated excellent recall for arches with the highest score among other elements in the NW facade, with almost all true positive points correctly identified. However, the low precision suggests significant misclassification, where arches were

confused with other curved elements. This indicates a need for enhanced parameters to reduce overlap between similar features.

Waterspouts Class

a. Accuracy: 88% (High)

b. Recall: 0% (Low)

c. Precision: 0% (Low)

d. FPR: 12% (Low)

Despite a high accuracy score, the classifier completely failed to identify waterspouts on the NW facade as shown in (Figure 4.4), as evidenced by the 0% recall and precision. The high accuracy is misleading and reflects the disproportionate number of waterspout points compared to the larger dataset, which heavily influenced the metric.

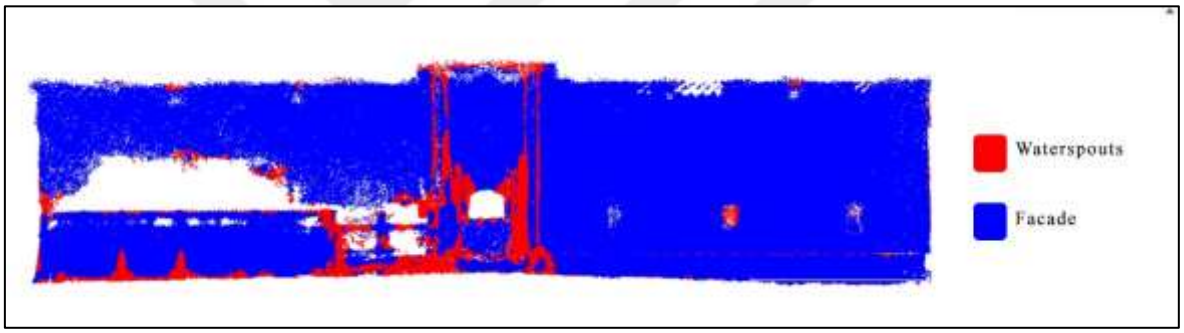

Figure 4.4: Segmentation Result of the Waterspouts Class from the Testing Dataset on the NW Facade.

For an overall view of CANUPO's classifier performance, Table 4.2 showcases the chosen classification results obtained from the data training and testing steps. Each result was categorized according to the set ranges of high, medium, and low accuracy. In the segmentation outcomes, the targeted element for segmentation is classified in red, while the facade is always classified in dark blue.

Table 4.2: Categorization of the Classification Results in High, Medium, and Low Accuracy, Based on the Accuracy Metric Percentages.

Accuracy Metric-Based Categorization		
High Accuracy (above 75%)	**Medium Accuracy (50 – 75%)**	**Low Accuracy (Below 50%)**
Southwestern Facade		
Main Load bearing walls Class 	Masonry Walls Class 	-
Columns Class 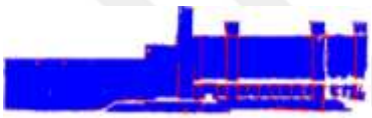	Windows Class 	-
Stairs Class 	Entrances Class 	-
Waterspouts Class 	Arches Class 	-
Northwestern Facade		
Stairs Class 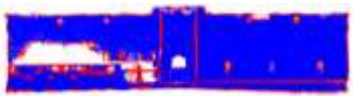	Masonry Walls Class 	-
Waterspouts Class 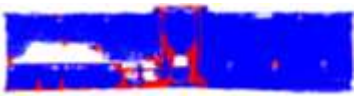	Windows Class 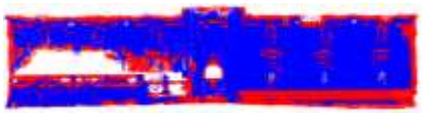	-

Table 4.2: Categorization of the Classification Results in High, Medium, and Low Accuracy, Based on the Accuracy Metric Percentages. (Table Continued)

-	Entrances Class 	-
-	Arches Class 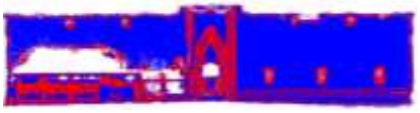	-

As seen in the table, the accuracy of most elements remains above 50%, and larger elements with a broader scale ramp like the main load-bearing walls, with a 1.1 min, 1.2 step, 2 max, and the columns from the SW facade, have a higher accuracy. On the other hand, the scale ramp with narrower values below 1 meter, had high and medium accuracy, yet no element resulted in a low accuracy from both facades. This categorization based on the accuracy metric alone gives a general insight into the classifier's performance without explanation of what was correctly identified as TP, what was correctly predicted, and what was correctly unclassified for the non-targeted elements. Therefore, analyzing the other evaluation metrics is essential. This further analysis of the highest and lowest performance for the classifier's detection of each element from the trained and testing data is proposed in Table 4.3.

Table 4.3: Categorization of the Fatih Mosque's Elements Based on the Classifier's Highest and Lowest Segmentation Performance on the SW Façade.

CANUPO's Highest Performance on the Trained Data from the SW Facade								
Evaluation Metric	**Class**							
	Masonry walls	Main Load Bearing Walls	Columns	Windows	Entrances	Stairs	Arches	Waterspouts
Accuracy								
Recall								

Table 4.3: Categorization of the Fatih Mosque's Elements Based on the Classifier's Highest and Lowest Segmentation Performance on the SW Facade. (Table Continued).

Precision								
FPR								
CANUPO's Lowest Performance on the Trained Data from the SW Facade								
Accuracy								
Recall								
Precision								
FPR								

This color-coded table compares the highest and lowest performance for the CANUPO's plugin on the trained data from the SW side. For the case of highest performance, waterspouts scored the highest results in three metrics including accuracy, precision, and FPR. While the masonry walls scored the highest performance with a 57% recall. Table 4.4 presents the same comparison but on the data used for testing captured from the NW façade.

Table 4.4: Categorization of the Fatih Mosque's Elements Based on the Classifier's Highest and Lowest Segmentation Performance on the NW Facade.

CANUPO's Highest Performance on the Testing Data from the NW Façade								
Evaluation Metric	**Class**							
	Masonry walls	Main Load Bearing Walls	Columns	Windows	Entrances	Stairs	Arches	Waterspouts
Accuracy								
Recall								
Precision								
FPR								

Table 4.4: Categorization of the Fatih Mosque's Elements Based on the Classifier's Highest and Lowest Segmentation Performance on the NW Facade. (Table Continued)

	CANUPO's Lowest Performance on the Testing Data from the NW Façade							
Accuracy								
Recall								
Precision								
FPR								

Similar to the results from the trained data, waterspouts scored the highest performance in the accuracy and FPR matrices. However, it didn't score the highest recall, but the arches elements did. And same to the trained data, masonry walls had the highest precision with 86%. In both facades, waterspouts scored the lowest performance for the precision matric, but on the NW façade, it had the lowest rate for the recall metric too. Similarly, both facades had the lowest performance for the FPR done on masonry walls.

Based on all of the findings' categorization and results, the next chapter discusses the meaning behind all the obtained results, what do they indicates, what statements they align or contradict with, and future implication and developments should be taken into account.

5. DISCUSSION AND CONCLUSION

The findings of this study provide valuable insights into the advantages and challenges faced by the utilization of the CANUPO classifier for the semantic segmentation of facade elements from heritage data. Also, it covers the effectiveness of using a photogrammetric approach for the capturing of Fatih mosque in Istanbul. Given the historical significance and value of the mosque, the production of reliable representation and segmentation is vital. This chapter describes the reliability of the results, reflecting on the methodological and assessment approaches, the effectiveness of CANUPO, and the impact of environmental factors on data collection and the classification results. Also, the study's limitations are discussed as well as future suggestions for developed implications of this study.

Sun lighting, which is a very important environmental factor for data collection, can affect the classification results massively. When the sun is strong and hits the building creating strong sharp shadows, this can lead to misclassifications, because it confuses the classifier into thinking that the shaded and unshaded areas have different materials. The classifier depends on the point's attributes such as textures and reflectivity. Therefore, when the sun hits the surface, the classifier falsely reads the point's attributes by thinking it has a darker or more reflective material when it doesn't. Also, it affects the point processing procedure, which limits the processing software's ability to fully identify the captured building features resulting in gaps within the points or uncompleted objects within the model. This occurred in the generation of the SW and NW facade, where the interior part of the windows is partially missing with fewer points number because the area has shadows and is darker than its surroundings, which resulted in partial gaps. However, this didn't occur because the sun was hitting but generally the window's interior goes deeper inside than the rest of the elements which resulted in a darker appearance. This aligns with the statement of (Arza-García et al., 2019) on the presence of shadows and how negatively it can affect the point cloud model's generation and segmentation outcomes. Regarding the lighting condition, this was taken into consideration during all the site visits to the Fatih mosque site. By visiting the site at 7 a.m. where no shadows were visible, Agisoft Metashape represented the captured buildings effectively. Considering the effects of environmental conditions, particularly sun lighting and shadow management, plays a vital role in the classifier's segmentation performance. Moreover, utilizing smartphones which are accessible to everyone showed that

it is quite a good data collection tool for capturing heritage buildings which resulted in good and considerable outcomes. This indicates that using accessible and cost-effective tools is sufficient without the need for high-end equipment This aligns with this study's intent to use an available, portable, and cost-effective data collection method.

The point cloud model's resolution is another important aspect in the field of heritage elements' semantic segmentation. Contrary to what was expected, producing a high quality point cloud model didn't make notable differences in the segmentation outcomes. Upon the trial mentioned in the methodology on producing a high-quality model of the SW façade which resulted in more than 10 million points, the classification outcomes weren't different from the one obtained from the medium-quality model. In the contrary, the classifier's training and classification time was significantly higher than the training and classification time on the SW façade. This employs that for large datasets like the Fatih mosque's façade, obtaining a high quality model isn't required especially if the time factor was a constraint. These findings suggest that extra details from high-quality models do not necessarily contribute to better classification performance.

The study also found that the segmentation results were influenced by the selection of scale ramp values in the training phase done on the SW façade, which is a crucial step that needs to be explored when working with the CANUPO classifier in CloudCompare. Experimentation with the maximum and step values showed the most effect in the classification outcomes on the SW side, where adjusting the maximum and step parameters improved CANUPO's ability to learn features and segment them on the trained data. However, adjusting the minimum scale parameter had minimal impact on the segmentation of smaller elements. Whether it was set to a higher value above 1 meter or a lower value of 20 cm, the results almost stayed the same, with minor changes for most of the elements. This might be improved in the case of segmenting smaller building elements, where the classifier analyzes smaller areas and captures finer detail. Accordingly, for the case of masonry walls and main load-bearing walls increasing the maximum scale parameter for larger elements resulted in higher recall values, as the classifier effectively conducted better analysis by analysing larger elements on larger areas. However, this study doesn't have a definite conclusion regarding this aspect because the elements within the study scope are relatively big, not focusing on the segmentation of ornaments and finer details.

Regarding the evaluation metrics results, which form the basis of this section on the utilized data interpretation methodology, the accuracy metric achieved with CANUPO ranged from high to medium, highlighting both positive and negative aspects of its application. For both facades of the training and testing datasets, the waterspout element scored the highest accuracy. This might be due to several reasons, the first reason being the targeted element's proportion in comparison to the nontargeted class. In the case of waterspouts, it is the smallest element within the façade, which helped the classifier learn its features more easily than the other elements because it has fewer details and covers a smaller portion of the whole point cloud model. Another reason might be its distinctive geometry, because it is extruded from the façade which helps CANUPO in distinguishing it better than other elements with closer points positions. Another pattern was recognized among the study's findings, which is the correlation between the accuracy and false positive rate metrics. In the case of the waterspout having the highest accuracy percentage from both facades, it also had the highest false positive rate percentage in both facades of the Fatih mosque. This suggests that accuracy is strongly influenced by the classifier's having lower attempts to misclassify the targeted element, which contributes to higher accuracy. However, high accuracy alone does not always suggest effective segmentation performance. While the classifier achieved 88% accuracy for the waterspout classification on the NW façade, it failed in the recall metric with a result of 0%. In contrast, on the SW façade, CANUPO achieved 91% accuracy and 98% recall for the waterspout, indicating successful segmentation. This variety in percentages suggests that CANUPO is heavily influenced by the spatial context and point density of the targeted element. Since this plugin was originally designed to segment vegetation and terrain, it showed a higher success with percentages near 98% within that field (Becker et al., 2024) (Štroner et al., 2021). However, in this study, it wasn't possible to obtain high accuracy across all elements.

Recall metrics further illustrate the classifier's inconsistent performance, revealing varied results across architectural elements. While some elements such as arches and columns showed relatively high recall values, others, smaller elements like the waterspouts from the testing dataset, had a 0% recall rate which questions the classification reliability. This recall outcome aligns with the findings from Moyano et al. (2021), which claimed that CANUPO detects larger elements better than smaller ones. Such inconsistencies in the accuracy percentages results indicate that CANUPO's effectiveness is not strictly dependent but may

also relate to point density and data uniformity across different façades. Moreover, the semantic segmentation of the column element from the trained dataset demonstrated reasonably high recall, suggesting an ability to detect large, continuous structures. Generally, the recall percentages on the trained data are higher than the recall percentages obtained from the testing data. This suggests that CANUPO performs better on the data that is used for both training and classification, rather than unseen data.

Precision scores, however, scored low percentages for most elements captured from the SW and NW facades. Suggesting an issue with CANUPO's ability to predict specific features within the complex and large point cloud model of the Fatih Mosque. Low precision indicates that the classifier frequently assigned negative points to the targeted elements which consist of true positive points, resulting in a significant number of misclassifications. This low performance might come from the lack of enough representative data points to represent each element's unique features and points' attributes. As a result, CANUPO's effectiveness in accurately classifying complex and large architectural features remains limited, questioning its applicability to other richly decorated heritage buildings. On a positive note, the classifier demonstrated a relatively low false positive rate for most of the elements, particularly in its predictions for non-target elements. This low false positive rate implies that CANUPO made fewer mistakes in classifying nontargeted, which highlights an area in its applicability to heritage structures. Nevertheless, improving precision is crucial for utilizing CANUPO in heritage documentation and preservation.

The reliability of this study is impacted by the methodological choice of using a smartphone camera for data collection. Despite its limitations, this approach utilizing a smartphone for data collection provided a considerable approach toward cost-effective, accessible heritage documentation. Smartphones provide images with lower quality than professional cameras and other data collection tools like laser scanners or drones, which would provide higher accuracy. However, this study successfully showcases that, even with cost-effective and easy-to-use technology, meaningful insights into semantic segmentation for heritage documentation are possible. This affordable approach can be particularly valuable for researchers who may not have access to advanced equipment. Another limitation lies in the method used for assessment, in which the number of GTP and TP was carefully but manually identified, causing some errors related to human intervention. Despite these limitations, the

study's outcomes provide an informative insight into semantically segmenting heritage elements using the CANUPO classifier. The potential of CANUPO to achieve relatively reliable segmentation results with accessible technology highlights its value in heritage documentation.

In conclusion, this study illustrates the functionality of the CANUPO classifier for the semantic segmentation of the Fatih Mosque's building elements. It provides a framework for obtaining a semantically segmented digital model using a photogrammetric technique to capture the exsisting mosque. The Fatih Mosque, which was built between 1462 and 1470 and designed by the Architect Atik Sinan, is one of Istanbul most valuable landmarks. Because it doesn't only represent an Islamic symbol, but it resembles a historic event of Istanbul conquering. In which the mosque was named after the conqueror Fatih Sultan Mehmet II, who conquered Istanbul and established the byzantine empire.

The historical significance of the mosque mainly goes back to its original structure which resembled the Turkish identity and early Ottoman architectural style. Unfortunately, the mosque was subjected to multiple strong earthquakes which resulted in the loss of the original mosque, where it completely collapsed beyond alteration or repair. This led to the reconstruction of the existing mosque which started in 1767 and ended in 1771. Given its historical significance, different studies explored the reasons behind the collapse of the original mosque focusing on the analysis of its structural system, soil condition, and building materials. Despite these efforts, there is limited literature on the current and original structure, and a significant gap on the utilization of advanced technology for its documentation and preservation. This study focused on the documentation and autonomous detection of the facade elements from the point cloud model of Fatih Mosque. By addressing this gap through the utilization of machine learning and advanced technology for data collection, processing, and interpretation, this study contributes to the conservation of Fatih mosque, by generating a sharable digital heritage model and establishing a digital framework for heritage data collection and classification.

The research utilized an affordable and accessible data collection tool using a smartphone camera for capturing the southwestern and northwestern facades of the Fatih Mosque. Upon data collection, a dense point cloud model was generated for each facade using Agisoft Metashape, a photogrammetry processing software. Then, the dataset was cleaned using

manual and automatic tools within the Agisoft Metashape and CloudCompare software. To specify the facade elements chosen for segmentation, an ontology map of all of the facade elements was created, with a focus on classifying main elements of the facade resulting in eight classes which are masonry walls, main load bearing walls, columns, stairs, windows, entrances, arches and waterspouts.

By utilizing CANUPO for semantic segmentation, the process started with training the classifier for elements' classification on the SW facade, by adjusting the scale ramp values to obtain the best classifier file with suitable parameters for each element. Then, the obtained classifier files were used to test the classifier's ability to detect the same targeted elements but from unseen data. To tackle all the segmentation results, the confusion matrix points including true positives, true negatives, false positives, and false negatives points in addition to the ground truth points were calculated either manually or according to specific equations. The resulting points number for each element was recorded to be used for the evaluation metrics assessment equation. The evaluation metrics equations included the calculation of the accuracy, recall, precision, and false positive rate, which all contribute to a better understanding of CANUPO's performance on heritage data.

The findings showed challenges, inconsistency, and moderate performance of the classifier for the point cloud semantic segmentation of the Fatih Mosque building elements. The results revealed how elements like scale ramp values, environmental conditions, model quality, points' density, and the element's geometry impact the segmentation results, offering guidance for future studies and potential improvements utilizing a photogrammetric technique in combination with CANUPO for data interpretation and building elements analysis. Despite the challenges and inconsistency of the results, the study provides a valuable framework for further exploration on CANUPO's applications within the heritage documentation and conservation sector.

Future research should focus on optimizing CANUPO for smaller architectural elements by focusing on single-element segmentation or testing CANUPO's performance on one element repeated across multiple heritage buildings with a similar architectural style. Also, based on the mixed outcomes, future studies should explore the effect of scaling values on elements of different sizes and levels of detail to identify optimal configurations that enhance accuracy across varying architectural elements. Such explorations could uncover a more precise

relationship between scale and an element attribute, ultimately improving segmentation consistency. Additionally, combining photogrammetric data with advanced capturing tools, such as drones and professional cameras, could enhance segmentation precision and detail, allowing for a better analysis of the CANUPO classifier functionality with heritage data. These tools could also support the integration of segmented elements into BIM software, enabling better conservation practices and parametric object extraction for preservation and education purposes. To conclude, this study presented a notable framework for the digitalization and semantic segmentation of heritage buildings' elements using CANUPO, offering a technological approach for the documentation and preservation of Turkey's heritage assets.

REFERENCES

Alshawabkeh, Y., & Baik, A. (2023). Integration of photogrammetry and laser scanning for enhancing scan-to-HBIM modeling of Al Ula heritage site. *Heritage Science*, *11*(1). https://doi.org/10.1186/s40494-023-00997-2

Alshawabkeh, Y., Baik, A., & Miky, Y. (2021). Integration of laser scanner and photogrammetry for heritage BIM enhancement. *ISPRS International Journal of Geo-information*, *10*(5), 316. https://doi.org/10.3390/ijgi10050316

Argiolas, R., Bagnolo, V., Cera, S., & Cuccu, S. (2022). VIRTUAL ENVIRONMENTS TO COMMUNICATE BUILT CULTURAL HERITAGE: A HBIM BASED VIRTUAL TOUR. *˜the œInternational Archives of the Photogrammetry, Remote Sensing and Spatial Information Sciences/International Archives of the Photogrammetry, Remote Sensing and Spatial Information Sciences*, *XLVI-5/W1-2022*, 21–29. https://doi.org/10.5194/isprs-archives-xlvi-5-w1-2022-21-2022

Abbate, E., Invernizzi, S., & Spanò, A. (2020). HBIM parametric modelling from clouds to perform structural analyses based on finite elements: a case study on a parabolic concrete vault. *Applied Geomatics*, *14*(S1), 79–96. https://doi.org/10.1007/s12518-020-00341-4

Andriasyan, M., Moyano, J., Nieto-Julián, J. E., & Antón, D. (2020). From point cloud data to building information modelling: An automatic parametric workflow for heritage. *Remote Sensing*, *12*(7), 1094.

Alshawabkeh, Y., El-Khalili, M., Almasri, E., Bala'awi, F., & Al-Massarweh, A. (2020). Heritage documentation using laser scanner and photogrammetry. The case study of Qasr Al-Abidit, Jordan. *Digital Applications in Archaeology and Cultural Heritage*, *16*, e00133.

Arza-García, M., Gil-Docampo, M., & Ortiz-Sanz, J. (2019). A hybrid photogrammetry approach for archaeological sites: Block alignment issues in a case study (the Roman camp of A Cidadela). *Journal of Cultural Heritage*, *38*, 195–203. https://doi.org/10.1016/j.culher.2019.01.001

Antón, D., Medjdoub, B., Shrahily, R., & Moyano, J. (2018). Accuracy evaluation of the semi-automatic 3D modeling for historical building information models.

International Journal of Architectural Heritage, *12*(5), 790–805. https://doi.org/10.1080/15583058.2017.1415391

Akyuz, T., Akyuz, S., & Gulec, A. (2015). Elemental and spectroscopic characterization of plasters from Fatih Mosque-Istanbul (Turkey) by combined micro-raman, Ftir and EDXRF techniques. *Spectrochimica Acta Part A: Molecular and Biomolecular Spectroscopy*, *149*, 744–750. https://doi.org/10.1016/j.saa.2015.05.015

Agisoft. (n.d.). *Metashape: Professional photogrammetry software*. Agisoft. Retrieved June 28, 2024, from https://www.agisoft.com/metashape/

Agirbas, A., Yildiz, G., & Sahin, M. (2022). Interrelation between grid systems and star polygons of muqarnas ground projection plans. *Heritage Science*, *10*(1). https://doi.org/10.1186/s40494-022-00647-z

Becker, D., Raddatz, L., Roussel, C., & Klonowski, J. (2024). Analysis methods for deformation detection using TLS and UAS data on the example of a landslide simulation. *International Journal of Geo-Engineering*, *15*(1). https://doi.org/10.1186/s40703-023-00203-z

Barrile, V., & Fotia, A. (2021). A proposal of a 3D segmentation tool for HBIM management. *Applied Geomatics*, *14*(S1), 197–209. https://doi.org/10.1007/s12518-021-00373-4

Banfi, F. (2021). The evolution of Interactivity, Immersion and Interoperability in HBIM: digital model uses, VR and AR for built Cultural Heritage. *ISPRS International Journal of Geo-information*, *10*(10), 685. https://doi.org/10.3390/ijgi10100685

Bianchini, C. (2020). A methodological approach for the study of Domes. *Nexus Network Journal*, *22*(4), 983–1013. https://doi.org/10.1007/s00004-020-00526-9

Banfi, F. (2020d). HBIM, 3D drawing and virtual reality for archaeological sites and ancient ruins. *Virtual Archaeology Review*, *11*(23), 16. https://doi.org/10.4995/var.2020.12416

Borg, B., Dunn, M., Ang, A., & Villis, C. (2020). The application of state-of-the-art technologies to support artwork conservation: Literature review. *Journal of Cultural Heritage*, *44*, 239–259. https://doi.org/10.1016/j.culher.2020.02.010

Biagini, C., Ottobri, P., Banti, N., & Bongini, A. (2020). Validation processes of H-BIM models: A case study. *IOP Conference Series: Materials Science and Engineering*, *949*(1), 012115. https://doi.org/10.1088/1757-899x/949/1/012115

Bacci, G., Bertolini, F., Bevilacqua, M. G., Caroti, G., Zaragoza, I. M., Martino, M., & Piemonte, A. (2019). HBIM METHODOLOGIES FOR THE ARCHITECTURAL RESTORATION. THE CASE OF THE EX-CHURCH OF SAN QUIRICO ALL'OLIVO IN LUCCA, TUSCANY. *˜the œInternational Archives of the Photogrammetry, Remote Sensing and Spatial Information Sciences/International Archives of the Photogrammetry, Remote Sensing and Spatial Information Sciences*, *XLII-2/W11*, 121–126. https://doi.org/10.5194/isprs-archives-xlii-2-w11-121-2019

Barbosa, M. D. C. J. (2018). *As-Built Building Information Modeling (BIM) Workflows: From Point Cloud Data to BIM* (Doctoral dissertation, Universidade de Lisboa (Portugal)).

Boardman, C., & Bryan, P. (2018). *3D laser scanning for heritage: Advice and guidance on the use of laser scanning in archaeology and architecture*. Historic England.

Baik, A. (2017). From point cloud to Jeddah Heritage BIM Nasif Historical House – case study. *Digital Applications in Archaeology and Cultural Heritage*, *4*, 1–18. https://doi.org/10.1016/j.daach.2017.02.001

Barbosa, M. J., Pauwels, P., Ferreira, V., & Mateus, L. (2016). Towards increased BIM usage for existing building interventions. *Structural Survey*, *34*(2), 168-190.

Brodu, N., & Lague, D. (2012). 3D terrestrial lidar data classification of complex natural scenes using a multi-scale dimensionality criterion: Applications in geomorphology. *ISPRS Journal of Photogrammetry and Remote Sensing*, *68*, 121–134. https://doi.org/10.1016/j.isprsjprs.2012.01.006

Beyen, K. (2008). Structural identification for post-earthquake safety analysis of the fat I˙H mosque after the 17 august 1999 Kocael I˙earthquake. *Engineering Structures*, *30*(8), 2165–2184. https://doi.org/10.1016/j.engstruct.2007.08.005

Berilgen, M. M. (2007). Evaluation of local site effects on earthquake damages of Fatih Mosque. *Engineering Geology*, *91*(2–4), 240–253. https://doi.org/10.1016/j.enggeo.2007.02.001

Clini, P., Mariotti, C., Angeloni, R., & Cádiz, J. M. (2024). ARCHITECTURAL HERITAGE DIGITAL REPRESENTATIONS FOR CONSERVATION STRATEGIES. *˜the œInternational Archives of the Photogrammetry, Remote Sensing and Spatial Information Sciences/International Archives of the Photogrammetry, Remote Sensing and Spatial Information Sciences*, *XLVIII-2/W4-2024*, 111–118. https://doi.org/10.5194/isprs-archives-xlviii-2-w4-2024-111-2024

Champion, E., & Rahaman, H. (2019). 3D Digital Heritage Models as sustainable scholarly resources. *Sustainability*, *11*(8), 2425. https://doi.org/10.3390/su11082425

Costantino, D., Pepe, M., & Restuccia, A. (2021). Scan-to-HBIM for conservation and preservation of Cultural Heritage building: the case study of San Nicola in Montedoro church (Italy). *Applied Geomatics*, *15*(3), 607–621. https://doi.org/10.1007/s12518-021-00359-2

Croce, V., Caroti, G., De Luca, L., Jacquot, K., Piemonte, A., & Véron, P. (2021). From the Semantic Point Cloud to heritage-building information modeling: A semiautomatic approach exploiting machine learning. *Remote Sensing*, *13*(3), 461. https://doi.org/10.3390/rs13030461

Chaudhry, S., Salido-Monzú, D., & Wieser, A. (2021). A modeling approach for predicting the resolution capability in terrestrial laser scanning. *Remote Sensing*, *13*(4), 615. https://doi.org/10.3390/rs13040615

Cotella, V. A. (2023). From 3D point clouds to HBIM: Application of Artificial Intelligence in Cultural Heritage. *Automation in Construction*, *152*, 104936. https://doi.org/10.1016/j.autcon.2023.104936

Charles, R. Q., Su, H., Kaichun, M., & Guibas, L. J. (2017). PointNet: Deep Learning on Point Sets for 3D Classification and Segmentation. *In Proceedings of the IEEE Conference on Computer Vision and Pattern Recognition*. https://doi.org/10.1109/cvpr.2017.16

CloudCompare. (n.d.). *CloudCompare: 3D point cloud and mesh processing software*. CloudCompare. Retrieved July 3, 2024, from https://www.danielgm.net/cc/

Colucci, E., De Ruvo, V., Lingua, A., Matrone, F., & Rizzo, G. (2020). HBIM-GIS integration: From IFC to CityGML standard for damaged cultural heritage in a

multiscale 3D GIS. *Applied Sciences*, *10*(4), 1356. https://doi.org/10.3390/app10041356

Damięcka-Suchocka, M., Katzer, J., & Suchocki, C. (2022). Application of TLS technology for documentation of brickwork heritage buildings and structures. *Coatings*, *12*(12), 1963. https://doi.org/10.3390/coatings12121963

Dorafshan, S., Thomas, R. J., Coopmans, C., & Maguire, M. (2019). A Practitioner's guide to small Unmanned aerial systems for bridge inspection. *Infrastructures*, *4*(4), 72. https://doi.org/10.3390/infrastructures4040072

Di Filippo, A., Sánchez-Aparicio, L. J., Barba, S., Martín-Jiménez, J. A., Mora, R., & Aguilera, D. G. (2018). Use of a wearable mobile laser system in seamless indoor 3D mapping of a complex historical site. *Remote Sensing*, *10*(12), 1897. https://doi.org/10.3390/rs10121897

Dostal, C., & Yamafune, K. (2018). Photogrammetric texture mapping: A method for increasing the Fidelity of 3D models of cultural heritage materials. *Journal of Archaeological Science: Reports/Journal of Archaeological Science: Reports*, *18*, 430–436. https://doi.org/10.1016/j.jasrep.2018.01.024

Dore, C., & Murphy, M. (2012). Integration of Historic Building Information Modeling (HBIM) and 3D GIS for recording and managing cultural heritage sites. *E. S. García, Et Al., Int. J. Sus. Dev. Plann.* https://doi.org/10.1109/vsmm.2012.6365947

Feroz, S., & Dabous, S. A. (2021). UAV-Based Remote sensing Applications for bridge condition assessment. *Remote Sensing*, *13*(9), 1809. https://doi.org/10.3390/rs13091809

Fan, H., Kong, G., & Zhang, C. (2021). An Interactive platform for low-cost 3D building modeling from VGI data using convolutional neural network. *Big Earth Data*, *5*(1), 49–65. https://doi.org/10.1080/20964471.2021.1886391

Guo, Y., Wang, H., Hu, Q., Liu, H., Liu, L., & Bennamoun, M. (2020). Deep learning for 3d point clouds: A survey. *IEEE transactions on pattern analysis and machine intelligence*, *43*(12), 4338-4364.

Guo, Y., Liu, Y., Oerlemans, A., Lao, S., Wu, S., & Lew, M. S. (2016). Deep learning for visual understanding: A review. Neurocomputing, 187, 27–48. https://doi.org/10.1016/j.neucom.2015.09.116

Galantucci, R. A., & Fatiguso, F. (2019). Advanced damage detection techniques in historical buildings using digital photogrammetry and 3D surface anlysis. *Journal of Cultural Heritage, 36*, 51–62. https://doi.org/10.1016/j.culher.2018.09.014

Grilli, E., Menna, F., & Remondino, F. (2017). A review of point clouds segmentation and classification algorithms. *The International Archives of the Photogrammetry, Remote Sensing and Spatial Information Sciences, XLII-2/W3*, 339–344. https://doi.org/10.5194/isprs-archives-xlii-2-w3-339-2017

Grilli, E., & Remondino, F. (2019). Classification of 3D digital Heritage. *Remote Sensing, 11*(7), 847. https://doi.org/10.3390/rs11070847

Grilli, E., Menna, F., & Remondino, F. (2017). A review of point clouds segmentation and classification algorithms. *The International Archives of the Photogrammetry, Remote Sensing and Spatial Information Sciences, 42*, 339-344.

Gines, J. L. C., & Cervera, C. B. (2019). Toward hybrid modeling and automatic planimetry for graphic documentation of the archaeological heritage: the Cortina Family Pantheon in the cemetery of Valencia. *International Journal of Architectural Heritage, 14*(8), 1210–1220. https://doi.org/10.1080/15583058.2019.1597214

Gurlitt, C. (1912). *Die baukunst konstantinopels. Textband*. Wasmuth.

Higueras, M., Calero, A. I., & Collado-Montero, F. J. (2021). Digital 3D modeling using photogrammetry and 3D printing applied to the restoration of a Hispano-Roman architectural ornament. *Digital Applications in Archaeology and Cultural Heritage, 20*, e00179.

Hackel, T., Savinov, N., Ladicky, L., Wegner, J. D., Schindler, K., & Pollefeys, M. (2017). SEMANTIC3D.NET: A NEW LARGE-SCALE POINT CLOUD CLASSIFICATION BENCHMARK. *ISPRS Annals of the Photogrammetry, Remote Sensing and Spatial Information Sciences, IV-1/W1*, 91–98. https://doi.org/10.5194/isprs-annals-iv-1-w1-91-2017

Hinton, G. E. (1990). CONNECTIONIST LEARNING PROCEDURES11This chapter appeared in Volume 40 of Artificial Intelligence in 1989, reprinted with permission of North-Holland Publishing. It is a revised version of Technical Report CMU-CS-87-115, which has the same title and was prepared in June 1987 while the author was at Carnegie Mellon University. The research was supported by contract N00014-86-K-00167 from the Office of Naval Research and by grant IST-8520359 from the National Science Foundation. In *Elsevier eBooks* (pp. 555–610). https://doi.org/10.1016/b978-0-08-051055-2.50029-8

Hu, Q., Yang, B., Xie, L., Rosa, S., Guo, Y., Wang, Z., Trigoni, N., & Markham, A. (2020). Randla-net: Efficient semantic segmentation of large-scale point clouds. *2020 IEEE/CVF Conference on Computer Vision and Pattern Recognition (CVPR)*. https://doi.org/10.1109/cvpr42600.2020.01112

Hamid-Lakzaeian, F. (2020). Point cloud segmentation and classification of structural elements in multi-planar masonry building facades. *Automation in Construction, 118*, 103232. https://doi.org/10.1016/j.autcon.2020.103232

Jovanović, D., Milovanov, S., Ruskovski, I., Govedarica, M., Sladić, D., Radulović, A., & Pajić, V. (2020). Building virtual 3D city model for smart cities applications: a case study on campus area of the University of Novi Sad. *ISPRS International Journal of Geo-information, 9*(8), 476. https://doi.org/10.3390/ijgi9080476

Jiang, M., Wu, Y., Zhao, T., Zhao, Z., & Lu, C. (2018, July 2). *PointSIFT: a SIFT-like network module for 3D point cloud semantic segmentation*. arXiv.org. https://arxiv.org/abs/1807.00652

Komarichev, A., Zhong, Z., & Hua, J. (2019). *A-CNN: Annularly convolutional neural networks on point clouds*. https://openaccess.thecvf.com/content_CVPR_2019/html/Komarichev_A-CNN_Annularly_Convolutional_Neural_Networks_on_Point_Clouds_CVPR_2019_paper.html

Koutsoudis, A., Ioannakis, G., Arnaoutoglou, F., Kiourt, C., & Chamzas, C. (2020). 3D reconstruction challenges using Structure-From-Motion. In *Advances in religious and cultural studies (ARCS) book series* (pp. 138–152). https://doi.org/10.4018/978-1-7998-2871-6.ch007

Kanun, E., Alptekin, A., & Yakar, M. (2021). Cultural heritage modelling using UAV photogrammetric methods: a case study of Kanlıdivane archeological site. *Advanced UAV, 1*(1), 24-33.

Kunter, H. B., & Ülgen, A. S. (1939a). *Fatih Camii ve Bizans Sarnıcı*.

Lou, L., Wei, C., Wu, H., & Yang, C. (2022). Cave feature extraction and classification from rockery point clouds acquired with handheld laser scanners. *Heritage Science, 10*(1). https://doi.org/10.1186/s40494-022-00810-6

Lowphansirikul, C., Kim, K., Vinayaraj, P., & Tuarob, S. (2019). 3D semantic segmentation of Large-Scale Point-Clouds in urban areas using deep learning. *3D Semantic Segmentation of Large-Scale Point-Clouds in Urban Areas Using Deep Learning*. https://doi.org/10.1109/kst.2019.8687813

Li, Z., & Shan, J. (2022). RANSAC-based multi primitive building reconstruction from 3D point clouds. *ISPRS Journal of Photogrammetry and Remote Sensing*, *185*, 247–260. https://doi.org/10.1016/j.isprsjprs.2021.12.012

Landrieu, L., & Simonovsky, M. (2018). Large-scale point cloud semantic segmentation with Superpoint graphs. *2018 IEEE/CVF Conference on Computer Vision and Pattern Recognition*. https://doi.org/10.1109/cvpr.2018.00479

Li, G., Muller, M., Thabet, A., & Ghanem, B. (2019). *DeepGCNS: Can GCNs go as deep as CNNs?* https://openaccess.thecvf.com/content_ICCV_2019/html/Li_DeepGCNs_Can_GCNs_Go_As_Deep_As_CNNs_ICCV_2019_paper.html

Martinelli, L., Calcerano, F., Adinolfi, F., Chianetta, D., & Gigliarelli, E. (2023). Open HBIM-IoT monitoring platform for the management of historical sites and museums. an application to the Bourbon Royal Site of Carditello. *International Journal of Architectural Heritage*, 1–18. https://doi.org/10.1080/15583058.2023.2272130

Moyano, J., León, J., Nieto-Julián, J. E., & Bruno, S. (2021). Semantic interpretation of architectural and archaeological geometries: Point cloud segmentation for HBIM parameterisation. *Automation in Construction, 130*, 103856. https://doi.org/10.1016/j.autcon.2021.103856

Malinverni, E. S., Pierdicca, R., Paolanti, M., Martini, M., Morbidoni, C., Matrone, F., & Lingua, A. (2019). DEEP LEARNING FOR SEMANTIC SEGMENTATION OF 3D POINT CLOUD. *˜the œInternational Archives of the Photogrammetry, Remote Sensing and Spatial Information Sciences/International Archives of the Photogrammetry, Remote Sensing and Spatial Information Sciences*, *XLII-2/W15*, 735–742. https://doi.org/10.5194/isprs-archives-xlii-2-w15-735-2019

Maru, M. B., Wang, Y., Kim, H., Yoon, H., & Park, S. (2023). Improved building facade segmentation through digital twin-enabled RandLA-Net with empirical intensity correction model. *Journal of Building Engineering*, *78*, 107520. https://doi.org/10.1016/j.jobe.2023.107520

Markiewicz, J., Tobiasz, A., Kot, P., Muradov, M., Shaw, A., & Al-Shammaa, A. (2019). Review of Surveying Devices for Structural Health Monitoring of Cultural Heritage Buildings. *Review of Surveying Devices for Structural Health Monitoring of Cultural Heritage Buildings*. https://doi.org/10.1109/dese.2019.00113

Moyano, J., Nieto-Julián, J. E., Lenin, L. M., & Bruno, S. (2021). Operability of point cloud data in an architectural Heritage information model. *International Journal of Architectural Heritage*, *16*(10), 1588–1607. https://doi.org/10.1080/15583058.2021.1900951

Mohammadi, M., Rashidi, M., Mousavi, V., Karami, A., Yu, Y., & Samali, B. (2021). Quality evaluation of digital twins generated based on UAV photogrammetry and TLS: Bridge case study. *Remote Sensing*, *13*(17), 3499.

Martínez-Carricondo, P., Carvajal-Ramírez, F., Yero-Paneque, L., & Agüera-Vega, F. (2021). Combination of HBIM and UAV photogrammetry for modelling and documentation of forgotten heritage. Case study: Isabel II dam in Níjar (Almería, Spain). *Heritage Science*, *9*(1), 95.

Murphy, M., McGovern, E., & Pavia, S. (2009). Historic building information modelling (HBIM). *Structural Survey*, *27*(4), 311–327. https://doi.org/10.1108/02630800910985108

Mateus, L., Fernández, J., Ferreira, V., Oliveira, C., Aguiar, J., Gago, A. S., ... & Pernão, J. (2019). Graphical data flow based in TLS and photogrammetry for consolidation

studies of historical sites. The case study of Juromenha fortress in Portugal. *The International Archives of Photogrammetry, Remote Sensing and Spatial Information Sciences*, *42*, 767-773.

Mol, A., Cabaleiro, M., Sousa, H. S., & Branco, J. M. (2020). HBIM for storing life-cycle data regarding decay and damage in existing timber structures. *Automation in Construction*, *117*, 103262.

Macher, H., Landes, T., & Grussenmeyer, P. (2017). From point clouds to building information models: 3D semi-automatic reconstruction of indoors of existing buildings. *Applied Sciences*, *7*(10), 1030. https://doi.org/10.3390/app7101030

Moyano, J., Justo-Estebaranz, Á., Nieto-Julián, J. E., Barrera, A. O., & Fernández-Alconchel, M. (2022). Evaluation of records using Terrestrial Laser Scanner in Architectural Heritage for information modeling in HBIM Construction: The case study of the la anunciación church (Seville). *Journal of Building Engineering*, *62*, 105190. https://doi.org/10.1016/j.jobe.2022.105190

Nieto, J. E., Moyano, J. J., Rico, F., & Antón, D. (2016). Management of built heritage via the HBIM Project: Acase study of flooring and wall tiling. Virtual Archaeology Review, 7, 14, 1–12.

Nespeca, R., Mariotti, C., Petetta, L., & Mandriota, A. (2024). POINT CLOUD SEGMENTATION IN HERITAGE PRESERVATION. ADVANCED DIGITAL PROCESS FOR HISTORICAL HOUSES. *˜the œInternational Archives of the Photogrammetry, Remote Sensing and Spatial Information Sciences/International Archives of the Photogrammetry, Remote Sensing and Spatial Information Sciences*, *XLVIII-2/W4-2024*, 325–332. https://doi.org/10.5194/isprs-archives-xlviii-2-w4-2024-325-2024

Nurunnabi, A., Belton, D., & West, G. (2012). Robust Segmentation in Laser Scanning 3D Point Cloud Data. *In Proceedings of the 2012 International Conference on Digital Image Computing Techniques and Applications (DICTA)*. https://doi.org/10.1109/dicta.2012.6411672

Oreni, D., Brumana, R., Della Torre, S., Banfi, F., Barazzetti, L., & Previtali, M. (2014). Survey turned into HBIM: the restoration and the work involved concerning the

Basilica di Collemaggio after the earthquake (L'Aquila). *ISPRS Annals of the Photogrammetry, Remote Sensing and Spatial Information Sciences*, *II–5*, 267–273. https://doi.org/10.5194/isprsannals-ii-5-267-2014

Opoku, D. J., Perera, S., Osei-Kyei, R., & Rashidi, M. (2021). Digital twin application in the construction industry: A literature review. *Journal of Building Engineering*, *40*, 102726. https://doi.org/10.1016/j.jobe.2021.102726

Penjor, T., Banihashemi, S., Hajirasouli, A., & Golzad, H. (2024). Heritage Building Information Modeling (HBIM) for Heritage Conservation: Framework of Challenges, gaps, and existing limitations of HBIM. *Digital Applications in Archaeology and Cultural Heritage*, *35*. https://doi.org/10.1016/j.daach.2024.e00366

Paiva, P. V. V., Cogima, C. K., Dezen-Kempter, E., & Carvalho, M. a. G. (2020). Historical building point cloud segmentation combining hierarchical watershed transform and curvature analysis. *Pattern Recognition Letters*, *135*, 114–121. https://doi.org/10.1016/j.patrec.2020.04.010

Pang, H. E., & Biljecki, F. (2022). 3D building reconstruction from single street view images using deep learning. *International Journal of Applied Earth Observation and Geoinformation*, *112*, 102859.

Pocobelli, D. P., Boehm, J., Bryan, P., Still, J., & Grau-Bové, J. (2018). Bim for heritage science: A Review. *Heritage Science*, *6*(1). https://doi.org/10.1186/s40494-018-0191-4

Qian, G., Li, Y., Peng, H., Mai, J., Hammoud, H. A. A. K., Elhoseiny, M., & Ghanem, B. (2022, October 12). *PointNeXt: Revisiting pointnet++ with improved training and scaling strategies*. arXiv.org. https://arxiv.org/abs/2206.04670

Quattrini, R., Malinverni, E. S., Clini, P., Nespeca, R., & Orlietti, E. (2015). FROM TLS TO HBIM. HIGH QUALITY SEMANTICALLY-AWARE 3D MODELING OF COMPLEX ARCHITECTURE. *˜the œInternational Archives of the Photogrammetry, Remote Sensing and Spatial Information Sciences/International Archives of the Photogrammetry, Remote Sensing and Spatial Information Sciences*, *XL-5/W4*, 367–374. https://doi.org/10.5194/isprsarchives-xl-5-w4-367-2015

Qi, C. R., Yi, L., Su, H., & Guibas, L. J. (2017). Pointnet++: Deep hierarchical feature learning on point sets in a metric space. *Advances in neural information processing systems*, *30*.

Rashidi, M., & Samali, B. (2020). Health monitoring of bridges using RPAs. In *Lecture notes in civil engineering* (pp. 209–218). https://doi.org/10.1007/978-981-15-8079-6_20

Rocha, G., Mateus, L., Fernández, J., & Ferreira, V. (2020). A Scan-to-BIM methodology applied to heritage buildings. *Heritage*, *3*(1), 47–67. https://doi.org/10.3390/heritage3010004

Rashidi, M., Mohammadi, M., Kivi, S. S., Abdolvand, M. M., Truong-Hong, L., & Samali, B. (2020). A Decade of Modern bridge monitoring using Terrestrial Laser Scanning: Review and future Directions. *Remote Sensing*, *12*(22), 3796. https://doi.org/10.3390/rs12223796

Risbøl, O., Briese, C., Doneus, M., & Nesbakken, A. (2015). Monitoring cultural heritage by comparing DEMs derived from historical aerial photographs and airborne laser scanning. *Journal of Cultural Heritage*, *16*(2), 202–209. https://doi.org/10.1016/j.culher.2014.04.002

Rabbani, T., Van Den Heuvel, F., & Vosselman, G. (2006). Segmentation of point clouds using smoothness constraints. *In International Archives of Photogrammetry, Remote Sensing and Spatial Information Sciences*, 248–253. https://www.isprs.org/proceedings/XXXVI/part5/paper/RABB_639.pdf

Remondino, F., Nocerino, E., Toschi, I., & Menna, F. (2017). A CRITICAL REVIEW OF AUTOMATED PHOTOGRAMMETRIC PROCESSING OF LARGE DATASETS. *˜the œInternational Archives of the Photogrammetry, Remote Sensing and Spatial Information Sciences/International Archives of the Photogrammetry, Remote Sensing and Spatial Information Sciences*, *XLII-2/W5*, 591–599. https://doi.org/10.5194/isprs-archives-xlii-2-w5-591-2017

Rebec, K. M., Deanovič, B., & Oostwegel, L. (2022). Old buildings need new ideas: Holistic integration of conservation-restoration process data using Heritage Building Information Modelling. *Journal of Cultural Heritage, 55*, 30-42.

Stober, D., Žarnić, R., Penava, D., Turkalj Podmanicki, M., & Virgej-Đurašević, R. (2018). Application of HBIM as a research tool for Historical Building Assessment. *Civil Engineering Journal*, *4*(7), 1565. https://doi.org/10.28991/cej-0309195

Shabani, A., Skamantzari, M., Tapinaki, S., Georgopoulos, A., Plevris, V., & Kioumarsi, M. (2022). 3D simulation models for developing Digital Twins of Heritage Structures: Challenges and strategies. *Procedia Structural Integrity*, *37*, 314–320. https://doi.org/10.1016/j.prostr.2022.01.090

Štroner, M., Urban, R., Lidmila, M., Kolář, V., & Křemen, T. (2021). Vegetation filtering of a steep rugged terrain: the performance of standard algorithms and a newly proposed workflow on an example of a railway ledge. *Remote Sensing*, *13*(15), 3050. https://doi.org/10.3390/rs13153050

Stouffs, R., & Tunçer, B. (2015). Typological descriptions as generative guides for historical architecture. *Nexus Network Journal*, *17*(3), 785–805. https://doi.org/10.1007/s00004-015-0260-x

Štroner, M., Urban, R., Lidmila, M., Kolář, V., & Křemen, T. (2021). Vegetation filtering of a steep rugged terrain: The performance of standard algorithms and a newly proposed workflow on an example of a railway ledge. *Remote Sensing*, *13*(15), 3050. https://doi.org/10.3390/rs13153050

Solla, M., Gonçalves, L. M., Gonçalves, G., Francisco, C., Puente, I., Providência, P., ... & Rodrigues, H. (2020). A building information modeling approach to integrate geomatic data for the documentation and preservation of cultural heritage. *Remote Sensing*, *12*(24), 4028.

Shen, Y., Feng, C., Yang, Y., & Tian, D. (2018). *Mining point cloud local structures by kernel correlation and graph pooling*. https://openaccess.thecvf.com/content_cvpr_2018/html/Shen_Mining_Point_Cloud_CVPR_2018_paper.html

Sun, X., Guo, B., Li, C., Sun, N., Wang, Y., & Yao, Y. (2024). Semantic segmentation and roof reconstruction of urban buildings based on LiDAR point clouds. *ISPRS International Journal of Geo-Information*, *13*(1), 19. https://doi.org/10.3390/ijgi13010019

Themistocleous, K., Ioannides, M., Tryfonos, G., Pritchard, D., Cliffen, H., Katiri, M., Jončić, N., Osti, G., Rigauts, T., Ripanti, F., & Anayiotos, A. (2022). HBIM for cultural heritage: The case study of panayia karmiotissa church. *Earth Resources and Environmental Remote Sensing/GIS Applications XIII*. https://doi.org/10.1117/12.2636331

Themistocleous, K., Evagorou, E., Mettas, C., & Hadjimitsis, D. G. (2022). The use of digital twin models to document cultural heritage monuments. *Earth Resources and Environmental Remote Sensing/GIS Applications XIII*, 13. https://doi.org/10.1117/12.2636332

Themistocleous, K., Agapiou, A., & Hadjimitsis, D. (2016). 3D DOCUMENTATION AND BIM MODELING OF CULTURAL HERITAGE STRUCTURES USING UAVS: THE CASE OF THE FOINIKARIA CHURCH. *˜the œInternational Archives of the Photogrammetry, Remote Sensing and Spatial Information Sciences/International Archives of the Photogrammetry, Remote Sensing and Spatial Information Sciences, XLII-2/W2*, 45–49. https://doi.org/10.5194/isprs-archives-xlii-2-w2-45-2016

Truong-Hong, L., & Lindenbergh, R. (2022). Extracting structural components of concrete buildings from laser scanning point clouds from construction sites. *Advanced Engineering Informatics*, *51*, 101490. https://doi.org/10.1016/j.aei.2021.101490

Vatan, M. (2018). *Conservation of cultural heritage in Turkey: Offprint IC MOS conservation of cultural heritage in Turkey*. Retrieved from https://www.researchgate.net/publication/325008611_CONSERVATION_OF_CULTURAL_HERITAGE_IN_TURKEY_OFFPRINT_IC_MOS_CONSERVATION_OF_CULTURAL_HERITAGE_IN_TURKEY

Wang, Y., Sun, Y., Liu, Z., Sarma, S. E., Bronstein, M. M., & Solomon, J. M. (2019). Dynamic Graph CNN for learning on point clouds. *ACM Transactions on Graphics*, *38*(5), 1–12. https://doi.org/10.1145/3326362

Wang, X., Liu, S., Shen, X., Shen, C., & Jia, J. (2019). *Associatively segmenting instances and semantics in point clouds*. https://openaccess.thecvf.com/content_CVPR_2019/html/Wang_Associatively_Segmenting_Instances_and_Semantics_in_Point_Clouds_CVPR_2019_paper.html

Wang, W., Yu, R., Huang, Q., & Neumann, U. (2018). *SGPN: Similarity Group Proposal Network for 3D Point Cloud Instance Segmentation*. https://openaccess.thecvf.com/content_cvpr_2018/html/Wang_SGPN_Similarity_Group_CVPR_2018_paper.html

Wang, Q., Sohn, H., & Cheng, J. C. (2016). Development of a mixed pixel filter for improved dimension estimation using AMCW laser scanner. *ISPRS Journal of Photogrammetry and Remote Sensing*, *119*, 246–258. https://doi.org/10.1016/j.isprsjprs.2016.06.004

Xie, Y., Tian, J., & Zhu, X. X. (2020). Linking points with labels in 3D: A Review of Point Cloud Semantic Segmentation. *IEEE Geoscience and Remote Sensing Magazine*, *8*(4), 38–59. https://doi.org/10.1109/mgrs.2019.2937630

Yastıklı, N., & Alkıs, Z. (2003). Documentation of cultural heritage by using digital close range photogrammetry. *CIPA Heritage Documentation*. Retrieved from https://www.cipaheritagedocumentation.org/wp-content/uploads/2018/11/Yast%C4%B1kl%C4%B1-Alk%C4%B1%C5%9F-Documentation-of-cultural-heritage-by-using-digital-close-range-photogrammetry.pdf

Yang, S., Hou, M., & Li, S. (2023). Three-Dimensional Point Cloud Semantic Segmentation for Cultural Heritage: A Comprehensive Review. *Remote Sensing*, *15*(3), 548. https://doi.org/10.3390/rs15030548

Yang, J., Zhang, Q., Ni, B., Li, L., Liu, J., Zhou, M., & Tian, Q. (2019). Modeling point clouds with self-attention and Gumbel subset sampling. *2019 IEEE/CVF Conference on Computer Vision and Pattern Recognition (CVPR)*. https://doi.org/10.1109/cvpr.2019.00344

Yi, L., Zhao, W., Wang, H., Sung, M., & Guibas, L. J. (2019). *GSPN: Generative Shape Proposal Network for 3D instance Segmentation in point Cloud*. https://openaccess.thecvf.com/content_CVPR_2019/html/Yi_GSPN_Generative_Shape_Proposal_Network_for_3D_Instance_Segmentation_in_CVPR_2019_paper.html

Zhao, H., Jiang, L., Jia, J., Torr, P., & Koltun, V. (2021). Point Transformer. *2021 IEEE/CVF International Conference on Computer Vision (ICCV)*. https://doi.org/10.1109/iccv48922.2021.01595

Zhao, H., Jiang, L., Fu, C., & Jia, J. (2019). PointWeb: Enhancing Local Neighborhood Features for Point Cloud Processing. *In Proceedings of the IEEE/CVF Conference on Computer Vision and Pattern Recognition*. https://doi.org/10.1109/cvpr.2019.00571

Zhang, J., Fukuda, T., & Yabuki, N. (2022). Automatic generation of synthetic datasets from a city digital twin for use in the instance segmentation of building facades. *Journal of Computational Design and Engineering*, *9*(5), 1737–1755. https://doi.org/10.1093/jcde/qwac086

Zou, Y., Weinacker, H., & Koch, B. (2021). Towards urban scene semantic segmentation with Deep Learning from lidar point clouds: A case study in Baden-Württemberg, Germany. *Remote Sensing*, *13*(16), 3220. https://doi.org/10.3390/rs13163220

Zhu, X. X., Tuia, D., Mou, L., Xia, G., Zhang, L., Xu, F., & Fraundorfer, F. (2017). Deep Learning in Remote Sensing: A comprehensive review and list of resources. *IEEE Geoscience and Remote Sensing Magazine*, *5*(4), 8–36. https://doi.org/10.1109/mgrs.2017.2762307

APPENDIX A

This section presents an in-depth explanation of the procedure done on the experimentation with the scale ramp values within the CANUPO classifier. The complete data on the obtained results is presented in Table A.1.

Table A.1: The Complete Data on CANUPO's Training Trails on the SW Facade, Based on Changing the Scale Ramp Min, Max, and Step Values. Only Scale Values Marked with an Asterisk (*) Symbol Were Used for Testing.

Class	Value	Segmentation Results		
Windows	Max	Min: 0.2, Step: 0.4, Max: 0.6 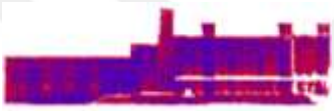	Min: 0.2, Step: 0.4, Max:0.8 * 	Min: 0.2, Step: 0.4, Max: 1.0 
	Step	Min: 0.2, Step: 0.3, Max: 0.8 	Min: 0.2, Step: 0.4, Max: 0.8 	Min: 0.2, Step: 0.6, Max: 0.8 
	Min	Min:0.08, Step: 0.4, Max: 0.8 	Min: 0.2, Step: 0.4, Max: 0.8 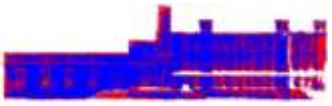	Min: 0.3, Step:0., Max: 0.8 
Masonry Walls	Max	Min:0.2, Step: 0.4, Max: 0.6 	Min: 0.2, Step: 0.4, Max: 0.8 	Min: 0.2, Step: 0.4, Max: 1.0 
	Step	Min: 0.2, Step: 0.3, Max: 0.8 	Min: 0.2, Step: 0.4, Max: 0.8 	Min: 0.2, Step: 0.6, Max:0.8 
	Min	Min: 0.08, Step:0.6, Max: 0.8	Min: 0.2, Step: 0.6, Max: 0.8 *	Min: 0.4, Step: 0.6, Max: 0.8

				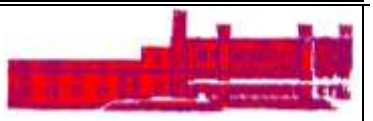
Columns	**Max**	Min: 0.2, Step: 0.6, Max: 1.0 	Min: 0.2, Step: 0.6, Max: 0.8 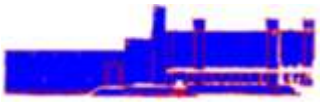	Min: 0.2, Step: 0.6, Max: 1.2 * 
	Step	Min: 0.2, Step: 0.6, Max: 1.2 	Min: 0.2, Step: 0.8, 1.2 	Min: 0.2, Step: 1.0, Max: 1.2 
	Min	Min: 0.2, Step: 0.8, Max: 1.2 	Min: 0.4, Step: 0.8, Max: 1.2 	Min: 0.6, Step: 0.8, Max: 1.2 
Stairs	**Max**	Min: 0.2, Step: 0.4, Max: 0.6 	Min: 0.2, Step: 0.4, Max: 0.8 * 	Min: 0.2, Step: 0.4, Max: 1.2 
	Step	Min: 0.2, Step: 0.4, Max: 0.8 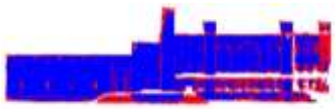	Min: 0.2, Step: 0.3, Max: 0.8 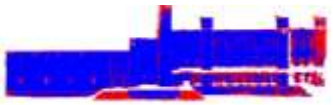	Min: 0.2, Step: 0.6, Max: 0.8 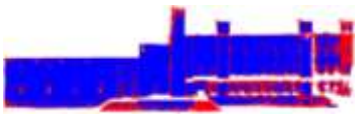
	Min	Min: 0.2, Step: 0.4, Max: 0.8 	Min: 0.08, Step: 0.4, Max: 0.8 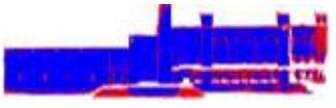	Min: 0.06, Step: 0.4, Max: 0.8 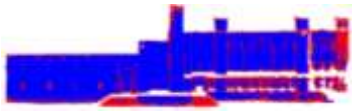
Main Load	**Max**	Min: 1.0, Step: 1.2, Max: 2 	Min: 1.0, Step: 1.2, Max: 1.6 	Min: 1.0, Step: 1.2, Max: 2.6 
		Min: 1.0, Step: 1.4, Max: 2.0	Min: 1.0, Step: 1.6, Max: 2.0	Min: 1.0, Step: 2.0, Max: 3.5

				
	Min	Min: 0.6, Step: 1.2, Max: 2 	Min: 0.8, Step: 1.2, Max: 2 	Min: 1.1, Step: 1.2, Max: 2 * 
Arches	**max**	Min: 0.2, Step: 0.4, Max: 0.6 	Min: 0.2, Step: 0.4, Max: 0.8 	Min: 0.2, Step: 0.4, Max: 1.0 
	step	Min: 0.2, Step: 0.3, Max: 0.8 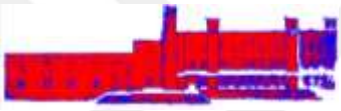	Min: 0.2, Step: 0.4, Max: 0.8 	Min: 0.2, Step: 0.6, Max: 0.8 
	min	Min: 0.08, Step: 0.4, Max: 0.8 	Min: 0.2, Step: 0.3, Max: 0.8 	Min: 0.3, Step: 0.4, Max: 0.8 * 
Entrances	**Max**	Min: 0.4, Step: 0.6, Max: 0.8 	Min: 0.4, Step: 0.6, Max: 1.2 	Min: 0.4, Step: 0.6, Max: 0.7 
	Step	Min: 0.4, Step: 0.5, Max: 0.8 	Min: 0.4, Step: 0.6, Max: 0.8 	Min: 0.4, Step: 0.7, Max: 0.8 * 
	Min	Min: 0.2, Step: 0.7, Max: 0.8 	Min: 0.4, Step: 0.7, Max: 0.8 	Min: 0.6, Step: 0.7, Max: 0.8 
Waters	**Max**	Min: 0.2, Step: 0.4, Max: 0.6 	Min: 0.2 Step: 0.4, Max: 0.8 	Min: 0.2, Step: 0.4, Max: 1.0 

	Step	Min: 0.2, Step: 0.4, Max: 1.0 * 	Min: 0.2, Step: 0.6, Max: 1.0 	Min: 0.2, Step: 0.8, Max: 1.0 
	Min	Min: 0.08, Step: 0.4, Max: 1.0 	Min: 0.2, Step: 0.4, Max: 1.0 	Min: 0.4, Step: 0.4, Max: 1.0 

This experiment was conducted to identify the role of the scale ramp value in the CANUPO's segmentation results. The minimum, maximum, and step parameters form the core of the CANUPO classifier. The main aim behind conducting this is to know which value has the most effect on the targeted elements and what pattern can be concluded. The method started by performing nine training and classification trails on each element. The 9 trials for each element can be grouped into three groups, with each group consisting of three experiments. the first group involves changing the maximum value only while keeping the minimum and step values constant. Then, the scale ramp values with the best classification result out of the first group is chosen. After that, the chosen values are explored in the second group. The second group also involved three experiments, where the step value was changed, and the minimum and maximum values were kept constant. Similarly, the scale ramp values with the best classification results from the second group is used to explore in the third group, which involves changing the minimum value while keeping the maximum and step values constant. In each experiment, the scale ramp value was changed, for example in the first experiment the maximum value was set to 0.6, then increased to 0.8, and the third time decreased to 0.4, while keeping the minimum and step parameters constant each time.

For most elements, a scale ramp value ranging between 0.2 to 0.8 meters was suitable for the classification on the trained dataset. However, for larger elements like the main load bearing walls and the columns, values above 1 meter were required to achieve optimal classification. This procedure helped in analyzing the classifier's performance based on the distances it analyses around each point.